evaluated the effect of anti-CD26 binding on Karpas 299 cell adhesion to the ECM and p38MAPK and integrin β_1 phosphorylation. We found that the anti-CD26 antibody 202.36 suppresses adhesion of Karpas 299 cells, whereas antibodies recognizing other CD26 epitopes display no inhibitory effect on cell adhesion (Fig. 4*A*). Of note is the fact that 202.36 does not affect cell viability at the dose and time tested (Fig. 4*B*). Furthermore, the inhibitory effect is in a dose-dependent manner (Fig. 4*C*). Importantly, we observed decreased phosphorylation of p38MAPK and integrin β_1 at the Thr^{180}/Tyr^{182} and Ser^{785} residues, respectively, following treatment with the anti-CD26 antibody 202.36 (Fig. 5).

CD26 depletion is associated with decreased tumorigenicity and increased survival in a severe combined immunodeficient mouse model. To investigate the effect of depletion of CD26 expression in an *in vivo* animal model, we inoculated mock and CD26-depleted clones into SCID mice i.p. and then monitored for tumor development and overall survival (Fig. 6). All of the mice inoculated with mock Karpas 299 clones developed tumor masses in the inguinal areas. The largest palpable tumor mass was monitored by serial measurements, and all the mice with tumors were eventually sacrificed per protocol. Importantly, none of the mice inoculated with CD26-depleted clones developed tumor masses over the observed time. Similar studies done with CD26-depleted clone 2 also showed no tumor development over similar times tested (data not shown).

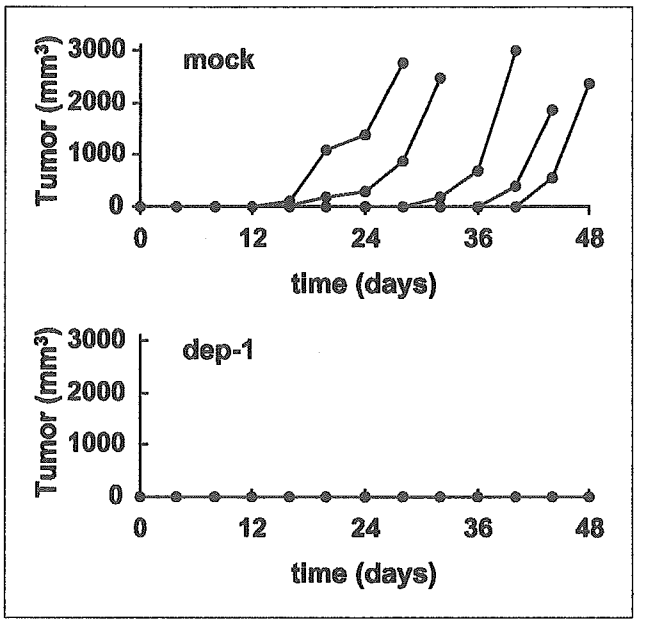

Figure 6. Effect of CD26 depletion on tumorigenicity in an *in vivo* SCID mouse model. SCID mice pretreated with anti–asialo-GM1 antibody were injected i.p. with mock or a CD26-depleted clone dep-1. The maximum diameter (MD) and transverse length (TL) of the largest inguinal mass were measured with a caliper, with tumor volume being calculated by the formula: MD × TL^2 × 1/2.

Discussion

In this article, we provide evidence linking CD26 to structures with important biological roles. We extend our previous studies by demonstrating the association between CD26 and topoisomerase IIα, with implications for the treatment of selected neoplasms with topoisomerase II inhibitors, such as doxorubicin. Importantly, our study is the first to report a linkage among CD26, p38MAPK, and integrin β_1. Our data indicate that CD26 is associated with integrin-dependent adhesion of Karpas 299 cells to the ECM by regulating p38MAPK-dependent phosphorylation of integrin β_1 at Ser^{785}. In addition, we show that down-regulation of CD26 expression decreases tumorigenicity of Karpas 299 cells in an *in vivo* SCID mouse xenograft model, hence suggesting that targeting CD26 may be an effective therapeutic strategy for selected neoplasms, specifically aggressive hematologic malignancies associated with high level of CD26 expression.

Previous work has suggested that CD26 may have a role in cell adhesion to ECM in selected experimental conditions (19, 22–24), although the mechanism involved with CD26 role in cell adhesion has not been clearly elucidated. Our present findings indicate that

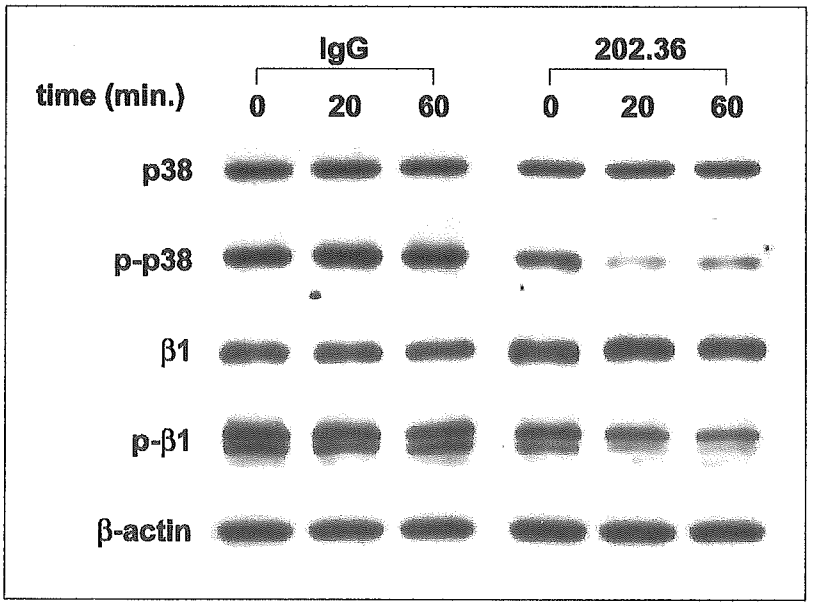

Figure 5. Effect of the anti-CD26 antibody 202.36 on phosphorylation of p38MAPK and integrin β_1. Karpas 299 cells were cultured with 10 μg/mL anti-CD26 antibody 202.36 or isotype control IgG for the indicated times. Levels of p38MAPK, phosphorylated p38MAPK at Thr^{180}/Tyr^{182}, integrin β_1, and phosphorylated integrin β_1 at Ser^{785} were evaluated by Western blotting as described in Materials and Methods, with each lane being loaded with equal amount of proteins and with β-actin as control.

the T-ALCL Karpas 299 cells bind to the ECM proteins fibronectin and collagen I and that this binding is regulated by CD26. Importantly, we show that CD26 affects ECM binding through integrin β_1 as supported by our data demonstrating that treatment with anti-integrin antibody inhibits binding of parental Karpas 299 to ECM and that the anti-CD26 antibody 202.36 also inhibits cell adhesion by suppressing phosphorylation of p38MAPK and integrin β_1 of Karpas 299. Furthermore, depletion of CD26 expression by siRNA transfection results in decreased integrin β_1 phosphorylation and inhibition of cell adhesion to ECM. Our data also suggest that the specific epitope recognized by the anti-CD26 antibody 202.36, which is also the HIV-1 gp120-binding domain of CD26 (25), is responsible for CD26 regulation of cell adhesion, as other anti-CD26 antibodies recognizing other epitopes do not affect ECM binding.

Previous studies showed the importance of phosphorylation of the Ser^{785} residue of integrin β_1 in cell adhesion, as substitution of serine to methionine or aspartate at position 785 results in loss of binding (21). Our work extends these data by demonstrating specifically that the phosphorylation status of integrin β_1 at Ser^{785} regulates integrin β_1–dependent cell adhesion. Of note is the fact that CD26 depletion does not have an effect on the phosphorylation status of integrin β_1 at Thr^{788}/Thr^{789} (data not shown), which has also been reported to regulate integrin β_1–dependent cell adhesion (26, 27). We also note that we consistently observe two bands on Western blotting with the particular antibody used to detect integrin β_1 phosphorylated at Ser^{785}. Although the exact reason for this observation is presently unclear, several potential explanations can be offered. It is possible that particular breakdown products are detected along with the full-length protein. Alternatively, the level of phosphorylation at Ser^{785} residues may differ for different integrin β_1 molecules, hence slightly altering the molecular weights of individual integrin β_1 molecule and resulting in the heterogeneous bands detected. It is also possible that variants of integrin β_1 exist in Karpas 299 cells that are phosphorylated at Ser^{785}, leading to the observation of multiple protein bands.

Our data show that CD26 regulates integrin β_1 phosphorylation of Karpas 299 cells through its effect on p38MAPK. However, the mechanism involved in p38MAPK regulation of the phosphorylation status of integrin β_1 remains to be elucidated. Of note is the fact that transfectional overexpression of CD26 on the human Burkitt B-cell lymphoma cell line Jiyoye results in increased phosphorylation of p38MAPK (12) but does not lead to an accompanying enhancement in phosphorylation of integrin β_1 or induction of cell adhesion (data not shown). It is presently unclear how p38MAPK is able to induce phosphorylation of integrin β_1 in the T-cell lymphoma line Karpas 299 but not in the B-cell lymphoma line Jiyoye cells. It is likely that p38MAPK regulation of integrin β_1 phosphorylation is dependent on other factors that exist in the T-cell line Karpas 299 but not in the B-cell line Jiyoye. Likewise, it is presently unclear as to how CD26 regulates p38 phosphorylation. Given the fact that CD26 is a serine protease capable of cleaving selected biological factors, it is possible that CD26 indirectly regulates p38 phosphorylation pathway via the activity of its cleaved substrates. In addition, because CD26 physically and functionally associates with molecules with key roles in signal transduction, including the tyrosine phosphatase CD45 (5), CD26 may have an effect on p38 phosphorylation through its associated molecules.

An important aim of our present study is to clarify the role of CD26 in regulating the malignant behavior of tumors as a marker of aggressive disease for selected subsets for T-cell malignancies (9, 10, 14), which may allow for the rational selection of CD26 as a potential target for novel therapy. Our *in vivo* data with SCID mouse xenografts conclusively show that depletion of CD26 expression on Karpas 299 cells results in loss of tumorigenicity and enhanced survival. It is likely that the inability to bind to the ECM as a result of CD26 depletion prevents tumor development in the animal model, given the fact that there is no difference in the rate of proliferation or the level of spontaneous cell death between CD26-positive and CD26-depleted Karpas 299 cells (data not shown). Given the fact that Karpas 299 is a T-ALCL cell line, it is interesting to note that in a study involving 8 cases of patients with T-ALCL, 5 of 8 (63%) cases were positive for CD26 expression (9). Taken together, our findings suggest that CD26 ability to regulate cell adhesion through p38MAPK-dependent phosphorylation of integrin β_1 plays a key role in tumorigenicity of the T-ALCL cells Karpas 299 and that treatment strategies targeting CD26 may be an effective therapeutic approach for selected CD26-bearing tumors, including aggressive T-cell malignancies.

Acknowledgments

Received 2/28/2005; revised 5/2/2005; accepted 5/18/2005.

Grant support: Japan Society for the Promotion of Science (T. Sato), Kanae Foundation for Life and Socio-Medical Science (T. Sato), M.D. Anderson Cancer Center Physician-Scientist Award (N.H. Dang), Gillson Longenbaugh Foundation (N.H. Dang), and Goodwin Funds (N.H. Dang).

The costs of publication of this article were defrayed in part by the payment of page charges. This article must therefore be hereby marked *advertisement* in accordance with 18 U.S.C. Section 1734 solely to indicate this fact.

References

1. Pro B, Dang NH. CD26/dipeptidyl peptidase IV and its role in cancer. Histol Histopathol 2004;19:1345–51.
2. Fox DA, Hussey RE, Fitzgerald KA, et al. Tal, a novel 105 KD human T cell activation antigen defined by a monoclonal antibody. J Immunol 1984;133:1250–6.
3. Dang NH, Torimoto Y, Deusch K, Schlossman SF, Morimoto C. Comitogenic effect of solid-phase immobilized anti-1F7 on human CD4 T cell activation via CD3 and CD2 pathways. J Immunol 1990;144:4092–100.
4. Dang NH, Torimoto Y, Sugita K, et al. Cell surface modulation of CD26 by anti-1F7 monoclonal antibody. Analysis of surface expression and human T cell activation. J Immunol 1990;145:3963–71.
5. Torimoto Y, Dang NH, Vivier E, Tanaka T, Schlossman SF, Morimoto C. Coassociation of CD26 (dipeptidyl peptidase IV) with CD45 on the surface of human T lymphocytes. J Immunol 1991;147:2514–7.
6. Asada Y, Aratake Y, Kotani T, et al. Expression of dipeptidyl aminopeptidase IV activity in human lung carcinoma. Histopathology 1993;23:265–70.
7. Aratake Y, Kotani T, Tamura K, et al. Dipeptidyl aminopeptidase IV staining of cytologic preparations to distinguish benign from malignant thyroid diseases. Am J Clin Pathol 1991;96:306–10.
8. Bauvois B, De Meester I, Dumont J, Rouillard D, Zhao HX, Bosmans E. Constitutive expression of CD26/dipeptidylpeptidase IV on peripheral blood B lymphocytes of patients with B chronic lymphocytic leukaemia. Br J Cancer 1999;79:1042–8.
9. Carbone A, Gloghini A, Zagonel V, et al. The expression of CD26 and CD40 ligand is mutually exclusive in human T-cell non-Hodgkin's lymphomas/leukemias. Blood 1995;86:4617–26.
10. Dang NH, Aytac U, Sato K, et al. T-large granular lymphocyte lymphoproliferative disorder: expression of CD26 as a marker of clinically aggressive disease and characterization of marrow inhibition. Br J Haematol 2003;121:857–65.
11. Torimoto Y, Dang NH, Tanaka T, Prado C, Schlossman SF, Morimoto C. Biochemical characterization of CD26 (dipeptidyl peptidase IV): functional comparison of distinct epitopes recognized by various anti-CD26 monoclonal antibodies. Mol Immunol 1992;29:183–92.
12. Yamochi T, Yamochi T, Aytac U, et al. Regulation of p38 phosphorylation and topoisomerase IIα expression in the B-cell lymphoma line Jiyoye by CD26/dipeptidyl peptidase IV (DPPIV), associated with enhanced *in vitro*

and *in vivo* sensitivity to doxorubicin. Cancer Res 2005; 65:1973–83.
13. Hansen MB, Nielsen SE, Berg K. Re-examination and further development of a precise and rapid dye method for measuring cell growth/cell kill. J Immunol Methods 1989;119:203–10.
14. Carbone A, Cozzi M, Gloghini A, Pinto A. CD26/dipeptidyl peptidase IV expression in human lymphomas is restricted to CD30-positive anaplastic large cell and a subset of T-cell non-Hodgkin's lymphomas. Hum Pathol 1994;25:1360–5.
15. Sato K, Aytac U, Yamochi T, et al. CD26/dipeptidyl peptidase IV enhances expression of topoisomerase IIα and sensitivity to apoptosis induced by topoisomerase II inhibitors. Br J Cancer 2003;89:1366–74.
16. Aytac U, Sato K, Yamochi T, et al. Effect of CD26/dipeptidyl peptidase IV on Jurkat sensitivity to G_2-M arrest induced by topoisomerase II inhibitors. Br J Cancer 2003;88:455–62.
17. Aytac U, Claret FX, Ho L, et al. Expression of CD26 and its associated DPPIV enzyme activity enhances sensitivity to doxorubicin-induced cell cycle arrest at G_2-M checkpoint. Cancer Res 2001;61: 7204–10.
18. Ishida R, Iwai M, Marsh KL, et al. Threonine 1342 in human topoisomerase IIα is phosphorylated throughout the cell cycle. J Biol Chem 1996;271: 30077–82.
19. Dang NH, Torimoto Y, Schlossman SF, et al. Human CD4 helper T cell activation: functional involvement of two distinct collagen receptors, 1F7 and VLA integrin family. J Exp Med 1990;172:649–52.
20. Elangbam CS, Qualls CW Jr, Dahlgren RR. Cell adhesion molecules—update. Vet Pathol 1997;34:61–73.
21. Mulrooney JP, Hong T, Grabel LB. Serine 785 phosphorylation of the β_1 cytoplasmic domain modulates β_{1A}-integrin-dependent functions. J Cell Sci 2001; 114:2525–33.
22. Cheng HC, Abdel-Ghany M, Pauli BU. A novel consensus motif in fibronectin mediates dipeptidyl peptidase IV adhesion and metastasis. J Biol Chem 2003;278: 24600–7.
23. Loster K, Zeilinger K, Schuppan D, Reutter W. The cysteine-rich region of dipeptidyl peptidase IV (CD26) is the collagen-binding site. Biochem Biophys Res Commun 1995;217:341–8.
24. Kikkawa F, Kajiyama H, Ino K, Shibata K, Mizutani S. Increased adhesion potency of ovarian carcinoma cells to mesothelial cells by overexpression of dipeptidyl peptidase IV. Int J Cancer 2003;105:779–83.
25. Herrera C, Morimoto C, Blanco J, et al. Comodulation of CXCR4 and CD26 in human lymphocytes. J Biol Chem 2001;276:19532–9.
26. Wennerberg K, Fassler R, Warmegard B, Johansson S. Mutational analysis of the potential phosphorylation sites in the cytoplasmic domain of integrin β_{1A}. Requirement for threonines 788–789 in receptor activation. J Cell Sci 1998;111:1117–26.
27. Stroeken PJ, van Rijthoven EA, Boer E, Geerts D, Roos E. Cytoplasmic domain mutants of β_1 integrin, expressed in β_1-knockout lymphoma cells, have distinct effects on adhesion, invasion and metastasis. Oncogene 2000;19:1232–8.

MOLECULAR AND CELLULAR BIOLOGY, Sept. 2005, p. 7743–7757 Vol. 25, No. 17
0270-7306/05/$08.00+0 doi:10.1128/MCB.25.17.7743–7757.2005

CD26 Mediates Dissociation of Tollip and IRAK-1 from Caveolin-1 and Induces Upregulation of CD86 on Antigen-Presenting Cells

Kei Ohnuma,[1] Tadanori Yamochi,[1,2] Masahiko Uchiyama,[1] Kunika Nishibashi,[1] Satoshi Iwata,[1] Osamu Hosono,[1] Hiroshi Kawasaki,[1] Hirotoshi Tanaka,[1] Nam H. Dang,[2] and Chikao Morimoto[1]*

Department of Clinical Immunology, Advanced Clinical Research Center, Institute of Medical Science, University of Tokyo, 4-6-1 Shirokanedai, Minato-ku, Tokyo 108-8639, Japan,[1] and Department of Lymphoma/Myeloma, M. D. Anderson Cancer Center, 1515 Holcombe Boulevard, Houston, Texas 77030[2]

Received 10 March 2005/Returned for modification 8 April 2005/Accepted 30 May 2005

CD26 is a T-cell costimulatory molecule with dipeptidyl peptidase IV enzyme activity in its extracellular region. We have previously reported that the addition of recombinant soluble CD26 resulted in enhanced proliferation of human T lymphocytes induced by the recall antigen tetanus toxoid (TT) via upregulation of CD86 on monocytes and that caveolin-1 was a binding protein of CD26, and the CD26–caveolin-1 interaction resulted in caveolin-1 phosphorylation (p-cav-1) as well as TT-mediated T-cell proliferation. However, the mechanism involved in this immune enhancement has not yet been elucidated. In the present work, we perform experiments to identify the molecular mechanisms by which p-cav-1 leads directly to the upregulation of CD86. Through proteomic analysis, we identify Tollip (Toll-interacting protein) and IRAK-1 (interleukin-1 receptor-associated serine/threonine kinase 1) as caveolin-1-interacting proteins in monocytes. We also demonstrate that following stimulation by exogenous CD26, Tollip and IRAK-1 dissociate from caveolin-1, and IRAK-1 is then phosphorylated in the cytosol, leading to the upregulation of CD86 via activation of NF-κB. Binding of CD26 to caveolin-1 therefore regulates signaling pathways in antigen-presenting cells to induce antigen-specific T-cell proliferation.

CD26 is a widely distributed 110-kDa cell surface glycoprotein with known dipeptidyl peptidase IV (DPPIV) (EC 3.4.14.5) activity in its extracellular domain (16, 38). This enzyme is capable of cleaving amino-terminal dipeptides with either L-proline or L-alanine at the penultimate position. While CD26 expression is enhanced following activation of resting T cells, $CD4^+$ $CD26^{high}$ T cells respond maximally to recall antigens such as tetanus toxoid (TT) (39). Cross-linking of CD26 and CD3 with solid-phase immobilized monoclonal antibodies (MAbs) can induce T-cell costimulation and interleukin-2 (IL-2) production by either human $CD4^+$ T cells or Jurkat T-cell lines transfected with CD26 cDNA (16, 56). In addition, anti-CD26 antibody treatment of T cells leads to a decrease in the surface expression of CD26 via its internalization, and such modulation results in an enhanced proliferative response to anti-CD3 or anti-CD2 stimulation as well as enhanced tyrosine phosphorylation of signaling molecules such as CD3ζ and p56-Lck (19). Moreover, we showed that DPPIV enzyme activity is required for CD26-mediated T-cell costimulation and various immune responses (23, 45, 58). We have recently shown that internalization of CD26 after cross-linking is mediated in part by the mannose-6-phosphate/insulin-like growth factor II receptor and that the interaction of CD26 and the mannose-6-phosphate/insulin-like growth factor II receptor plays a role in CD26-induced T-cell costimulation (20).

* Corresponding author. Mailing address: Division of Clinical Immunology, Advanced Clinical Research Center, Institute of Medical Science, University of Tokyo, 4-6-1 Shirokanedai, Minato-ku, Tokyo 108-8639, Japan. Phone: 81-354-495-546. Fax: 81-354-495-448. E-mail: morimoto@ims.u-tokyo.ac.jp.

In a recent study, we demonstrated that caveolin-1 is a binding protein of CD26 and that CD26 on activated memory T cells interacts with caveolin-1 on TT-loaded monocytes (43). In this interaction, the scaffolding domain (SCD) of caveolin-1, comprising residues 82 to 101, is associated with the caveolin binding domain (CBD) of CD26, comprising residues 201 to 211. Caveolin-1 was first identified as a major tyrosine-phosphorylated protein in v-Src-transformed chicken embryo fibroblasts (18). Multiple lines of evidence now suggest that caveolin-1 acts as a scaffolding protein capable of directly interacting with and modulating the activity of caveolin-bound signaling molecules. In support of this hypothesis, caveolin-1 binding can functionally modulate the activity of G-protein-coupled protein, membrane protein, nonreceptor tyrosine kinase, and nonreceptor serine/threonine kinases such as H-Ras, Src family kinases, protein kinase C isoforms, epidermal growth factor receptor, and endothelial nitric oxide synthetase (48). Caveolin-1 is the principal structural protein of caveolae and plays a role in the vesicular transport system, including lipid homeostasis, cell cycle regulation, apoptosis, and the regulation of signal transduction pathways (48, 51). In immune cells, caveolin-1 expressed on monocytes/macrophages helps to regulate scavenged lipids (28). Recently, we identified caveolin-1 on antigen-presenting cells (APC) as a binding protein for CD26 and demonstrated that CD26 stimulation upregulates surface expression of CD86 on APC by means of caveolin-1 and enhances TT-mediated T-cell proliferation (43). However, the signaling pathways resulting from CD26-mediated phosphorylation of caveolin-1 (p-cav-1) that lead to the eventual upregulation of CD86 in APC still remain to be elucidated.

In the present paper, we undertook studies to define the

molecular mechanisms by which p-cav-1 leads directly to the upregulation of CD86. We identify Tollip (Toll-interacting protein) and IRAK-1 (IL-1 receptor [IL-1R]-associated serine/threonine kinase 1) as caveolin-1-interacting proteins in APC through proteomic analysis. We demonstrate that binding of exogenous CD26 to APC results in the phosphorylation of caveolin-1 and dissociation of Tollip and IRAK-1 from caveolin-1 in the membrane of APC. Furthermore, following dissociation from caveolin-1 in the cell membrane, IRAK-1 is phosphorylated in the cytoplasm, leading eventually to the upregulation of CD86 through NF-κB activation. CD26 therefore enhances antigen-specific T-cell proliferation by engaging signaling pathways of APC through its interaction with caveolin-1.

MATERIALS AND METHODS

Cells, antibodies, and reagents. HEK293 human embryonal kidney, COS-7 monkey fibroblast, and THP-1 human monocyte cell lines were grown as described previously (43). Human peripheral monocytes were purified from peripheral blood mononuclear cells using a MACS Monocyte Isolation Kit II (Miltenyi), collected from healthy adult volunteers who were immunized with TT within 1 year before donation, and incubated according to the methods described previously (42). Informed consent was obtained from healthy adult volunteers. To avoid the effect of lipopolysaccharide (LPS) contamination, polymyxin B sulfate (20 IU/ml; Sigma-Aldrich) was added in all monocyte-containing cultures.

Anti-caveolin-1 rabbit polyclonal antibody (PAb), anti-IRAK rabbit PAb, anti-IκBα MAb, anti-glutathione-*S*-transferase (GST) MAb, antihemagglutinin (anti-HA) MAb, and anti-HA rabbit PAb agarose-conjugated antibodies were purchased from Santa Cruz Biotechnology Inc.; anti-phospho-caveolin-1 MAb was from BD Transduction; anti-Tollip rat MAb was from ALEXIS Biochemicals; anti-vesicular stomatitis virus (VSV) rabbit PAb was from Medical & Biological Laboratory Co. Ltd.; and anti-FLAG (M2) MAb, 3× FLAG peptide, and poly-L-lysine were from Sigma-Aldrich. Polystyrene latex beads (Molecular Probes) conjugated with recombinant soluble CD26 (rsCD26) were prepared as described previously (42, 43).

Constructions of plasmids. HA–caveolin-1 and caveolin-1–enhanced green fluorescent protein (GFP) were made by inserting caveolin-1 cDNA into pCG-N-BL and pEB6-CAG-EGFP (a kind gift from Yoshihiro Miwa) vectors, respectively (55, 61). A series of caveolin-1 deletion mutants were made by inserting cDNA fragments of mutated caveolin-1 generated by PCR. FLAG-Tollip and VSV–IRAK-1 were made by inserting Tollip cDNA into pFLAG-CMV-2 (Sigma) and pCORON1000 VSV-G (Amersham Biosciences), respectively. GST–caveolin-1 and luciferase chimera of the 5′-flanking region of the human CD86 gene were previously constructed in our laboratory as described elsewhere previously (43). All constructs or cDNA fragments were confirmed by DNA sequencing.

2D-PAGE. The membrane fraction from monocytes stimulated by rsCD26-coated polystyrene beads was extracted with a ReadyPrep protein extraction kit (Bio-Rad) according to the manufacturer's instructions. Membrane proteins were then cleaned up to pellets with a two-dimensional (2D) Clean-Up kit (Bio-Rad) and resuspended in rehydration lysis buffer {8 M urea, 2 M thiourea, 4% 3-[(3-cholamidopropyl)-dimethylammonio]-1-propanesulfonate (CHAPS), 50 mM dithiothreitol, 0.5% ZOOM carrier ampholyte (pH range, 3 to 10) (Invitrogen), 0.002% bromphenol blue} to a final concentration of 1 mg/ml. Wide-range immobilized pH gradient strips (pH 3-10NL; Invitrogen) were rehydrated in 155 μl of rehydration lysis buffer containing 50 μg protein and isoelectric focused at 1,367 V · h on a ZOOM IPGRunner system (Invitrogen). Second-dimension sodium dodecyl sulfate-polyacrylamide gel electrophoresis (SDS-PAGE) was performed using 4 to 12% NuPAGE bis-Tris gels (Invitrogen). Analytical gels were stained with colloidal Coomassie brilliant blue R250. Peptide mass mapping was performed by recording peptide mass fingerprints of typical in-gel digests of the corresponding gel spots using matrix-assisted laser desorption ionization–time of flight mass spectrometry (MALDI-TOF MS) (AXIMA-CFR plus; Shimadzu Biotech) and by subsequently searching the MASCOT database (Matrix Sciences).

Coprecipitation and immunoblotting. To study the interaction among endogenous caveolin-1, Tollip, and IRAK-1, lysates of monocytes were prepared using radioimmunoprecipitation assay lysis buffer as described previously (21, 27, 43). Following preclearing by control immunoglobulins (Igs), immunoprecipitations (IPs) were performed by incubating lysates with specific antibodies followed by the addition of protein G-Sepharose beads. Beads were then submitted to SDS-PAGE and Western blot analysis. To examine the interacting domains with fusion proteins, COS cells were transfected with HA–caveolin-1-, FLAG-Tollip-, and VSV–IRAK-1-expressing plasmids. IPs with these cell lysates and Western blotting were performed as described elsewhere previously (21, 27, 43).

Confocal laser microscopy. For fluorescent microscopy experiments using monocytes, cells were treated and stained according to methods described previously (42, 43). For fluorescent microscopy experiments using HEK293 cells, cells were preincubated in LAB-TEK 4-well chamber slide glass (Nalgen Nunc International). GFP–caveolin-1 or HA–caveolin-1, FLAG-Tollip, and VSV–IRAK-1 constructs were transfected using Lipofectamine 2000 reagent (Invitrogen). Cells were then washed with ice-cold phosphate-buffered saline (PBS), fixed in ice-cold 50% acetone in methanol, and incubated with anti-FLAG (M2) or anti-VSV antibodies. After being washed with ice-cold 5% bovine serum albumin–PBS, cells were stained with specific secondary antibodies, followed by mounting with an Antifade Prolong kit (Molecular Probes).

Luciferase assay. HEK293 cells were used to assay for human CD86 promoter activity following CD26–caveolin-1 interaction with Tollip and IRAK-1. Luciferase enzyme activity was determined using a luminometer (Promega), and relative light units were normalized to the protein amount determined with protein assay reagent according to the manufacturer's instructions (Pierce Biotechnology) (22, 32, 43).

Nuclear protein extraction and DNA-binding protein assay. Nuclear extracts were prepared from purified monocytes with indicated stimulations, and enzyme-linked immunosorbent assay (ELISA)-based DNA-binding protein assays were performed using Mercury TransFactor kits (BD Biosciences) as described previously (43).

siRNA against human Tollip and IRAK-1. We selected two target sequences from positions +186 to +206 (ss1) and +774 to +794 (ss2) downstream of the start codon of human Tollip mRNA (sense 1 small interfering RNA [siRNA] [ss1-siRNA], 5′-AAGTTGGCCAAGAATTACGGCdTdT; sense 2 siRNA [ss2-siRNA], 5′-AACAAGGATCCGCCATCAACdTdT). Moreover, mismatched siRNA (mis-siRNA) at 4 nucleotides was prepared to examine nonspecific effects of siRNA duplexes (mis-siRNA, 5′-UAGTTCGCCAAGTATTACCGCdTdT). siRNA targeting for human IRAK-1 was selected from positions +969 to +989 (ss3) downstream of the start codon of human IRAK-1 mRNA (5′-CCGGGC AATTCAGTTTCTACAdTdT). These selected sequences were also submitted to a BLAST search against the human genome sequence to ensure that only one gene of the human genome was targeted. siRNAs were purchased from QIAGEN. Transfection of siRNA into monocytes was conducted using the HVJ-E vector (GenomeONE; kindly provided by Ihsihara Sangyo Kaisha Ltd.) as described previously (43).

Cell labeling, culture conditions, and flow cytometric analysis. For T-cell proliferation assay, 1×10^6 cells/ml in PBS were labeled with an equal volume of 5 μM carboxyfluorescein diacetate succinimidyl ester according to the manufacturer's instructions (Molecular Probes). Unbound carboxyfluorescein diacetate succinimidyl ester, or the deacetylated form, carboxyfluorescein succinimidyl ester (CFSE), was quenched by the addition of an equal volume of heat-inactivated fetal calf serum. Analysis of cells immediately following CFSE labeling indicates a labeling efficiency that exceeds 99%, and all cells remained labeled for at least a 7-day period during cell culture. The labeled T cells were plated at 1×10^5 cells/well in round-bottomed 96-well microtiter plates with suspension in AIM-V medium (GIBCO), and T-cell activation was achieved by the addition of soluble anti-CD3 antibody (OKT3, 0.05 μg/ml) plus phorbol 12-myristate 13-acetate (PMA) (10 ng/ml), or T cells were plated with 1.0×10^4 cells/well of monocytes from the same donor, which were pretreated with or without TT and siRNA as described above. After a 96-h incubation, T-cell proliferation was analyzed by cell division of the $CD3^+$ subset of CFSE fluorescence using FACSCalibur and CellQuest Pro software (Becton-Dickinson).

Statistics. Student's *t* test was used to determine whether the difference between control and sample was significant (with a P value of <0.05 being significant).

RESULTS

Identification of differential membrane protein expression in CD26-stimulated monocytes. To explore signaling events in TT-loaded monocytes stimulated by CD26, we characterized changes in the expression levels of proteins found in the monocyte membrane. For this purpose, TT-loaded monocytes were

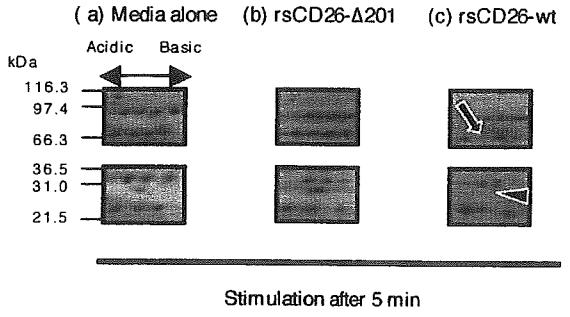

FIG. 1. 2D analysis of membrane proteins extracted from monocytes. Freshly isolated monocytes were pulsed with tetanus toxoid and stimulated with polystyrene latex beads coated with rsCD26-wt or rsCD26 deletion mutant at residues 201 to 211 (rsCD26-Δ201). Following stimulation for 0, 0.5, 5, 10, and 15 min, membrane proteins were extracted from these cells and then separated by 2D-PAGE using pH 3.0-10NL (nonlinear) immobilized pH gradients in the first dimension and 4 to 12% SDS-PAGE and stained with Coomassie brilliant blue 250R. Two spots clearly reduced or disappeared in monocytes undergoing a 5-min stimulation of rsCD26-wt as demonstrated in the figure (arrow and arrow head). Protein spots were identified using MALDI-TOF MS. The protein with a higher molecular mass was determined to be IRAK-1, with the other protein being Tollip. Similar results were obtained in five independent experiments, and the panels shown are the representative results.

stimulated with rsCD26-coated polystyrene latex beads (43). Membrane proteins of TT-loaded monocytes that were either unstimulated or stimulated with wild-type rsCD26 (rsCD26-wt)- or rsCD26-Δ201 (deleting CBD at residues 201 to 210)-coated beads were harvested at various periods and separated by 2D-PAGE as described in Materials and Methods. As shown in Fig. 1, an obvious decrease or disappearance of two spots in 2D-PAGE gel was observed after a 5-min stimulation by rsCD26-wt but not by rsCD26-Δ201. To define the two proteins found to be reduced by rsCD26-wt stimulation, the compatible spots in gels treated with medium alone and rsCD26-Δ201 were excised and analyzed by MALDI-TOF MS for protein identification. Proteins displaying a significant change in response to rsCD26-wt were found to be IRAK-1 (solid arrow in Fig. 1) and Tollip (arrowhead in Fig. 1).

IRAK-1 and Tollip interact with caveolin-1 in the membrane of monocytes. To further determine the protein-protein interaction among caveolin-1, IRAK-1, and Tollip in monocytes, we conducted IP studies using lysates of TT-loaded monocytes. As shown in Fig. 2A, IRAK-1 and caveolin-1 were precipitated with anti-Tollip antibody (lane 2, top and bottom panels). Moreover, Tollip and caveolin-1 were precipitated by anti-IRAK-1 antibody (lane 4, middle and bottom panels). To confirm this interaction, immunocytochemical analysis of monocytes was performed. As shown in Fig. 2B, caveolin-1 was located in the cell surface membrane and perinuclear area of monocytes (panels a and d), and Tollip and IRAK-1 were stained in the cell surface membrane and cytosol (b and g and e and h, respectively). Caveolin-1 and Tollip were colocalized in the cell surface membrane (Fig. 2B, panel c), and caveolin-1 and IRAK-1 were colocalized in the cell surface membrane as well (panel f). Moreover, as reported previously by other investigators (5, 62), Tollip and IRAK-1 were clearly merged with each other (Fig. 2B, panel i). These data strongly suggest that certain numbers of IRAK-1 and Tollip molecules found in monocytes are located in the cell surface membrane with caveolin-1.

We next focused on caveolin-1-mediated signaling events that upregulate CD86 expression following CD26 binding to caveolin-1 on TT-loaded monocytes. As shown in Fig. 2C (panel a), 0.5 to 10 min following stimulation with rsCD26-wt-coated beads, caveolin-1 in the membrane fraction was phosphorylated as reported previously (43). To clarify the comparison of protein expression levels, the changes in intensity of p-cav-1 were shown as a bar graph in Fig. 2C (panel h, solid bars). IRAK-1 and Tollip were found in IP complexes with caveolin-1 PAb at 0- to 0.5-min periods and were dissociated from caveolin-1 at 2 to 10 min following CD26–caveolin-1 interaction (Fig. 2C, panels b and c and light and dark gray bar graphs in panel h, respectively). Of note is that the expression of caveolin-1 was not affected by CD26 stimulation (Fig. 2C, panel d and open bar graphs in panel h). At these time points, IRAK-1 was found to be hyperphosphorylated by Western blot analysis of total lysates (Fig. 2C, panel e). The protein level of Tollip was not changed (Fig. 2C, panel f). In the previous study, we had observed activation of NF-κB in inducing upregulation of CD86 in response to CD26–caveolin-1 interaction (43). We therefore examined the potential involvement of NF-κB in caveolin-1-mediated signaling events that lead to the upregulation of CD86 expression following CD26 binding to caveolin-1 on TT-loaded monocytes. For this purpose, total cell lysates were used to evaluate the degradation of IκBα. As shown in Fig. 2C (panels g and h), IκBα was decreased at 2 to 10 min following CD26–caveolin-1 interaction (dark gray bar graphs in Fig. 2C, panel h). On the other hand, caveolin-1 was not phosphorylated after stimulation with mutant CD26 (rsCD26-Δ201) beads. Similarly, neither release of Tollip nor shift of IRAK was observed (data not shown). These results strongly suggest that the Tollip–IRAK-1–NF-κB cascade was triggered by CD26–caveolin-1 interaction.

Identification of binding domains among caveolin-1, Tollip, and IRAK-1. To further determine the binding domains involved in the caveolin-1–Tollip–IRAK-1 interaction, we constructed a series of GST- or HA-tagged caveolin-1, GST- or FLAG-tagged Tollip, and VSV-tagged IRAK-1 mutants (Fig. 3A). To determine the binding domains involved in the Tollip–caveolin-1 interaction, we first performed a GST pull-down assay using a series of GST-fused caveolin-1 with lysates of THP cells by the same methods described previously (43). As shown in Fig. 3B, Tollip was coprecipitated with GST-tagged wild-type caveolin-1 (GST–Cav-1-wt), Cav-1–N-terminal region (NT)+SCD, and Cav-1–ΔNT (lanes 1, 3, and 5) but not with GST-Cav-NT, Cav-ΔNTΔSCD, and Cav-ΔSCD (lanes 2, 4, and 6), implying that the SCD (residues 82 to 101) of caveolin-1 was required for binding to Tollip. Next, the binding domains of Tollip to caveolin-1 were determined. As shown in Fig. 3C, caveolin-1 was coprecipitated with GST-Tollip-wt, Tollip (protein kinase C conserved region 2 [C2] plus coupling of ubiquitin-conjugation to endoplasmatic reticulum-degradation domain [CUE]), Tollip-ΔCUE, and Tollip-C2 (lanes 1, 2, 3, and 7) but not with GST-Tollip-ΔC2ΔCUE, Tollip-CUE, and Tollip-ΔC2 (lanes 4, 5, and 6). These results revealed that the C2 domain of Tollip (residues 47 to 178) was associated with caveolin-1 interaction. Furthermore, series of FLAG-

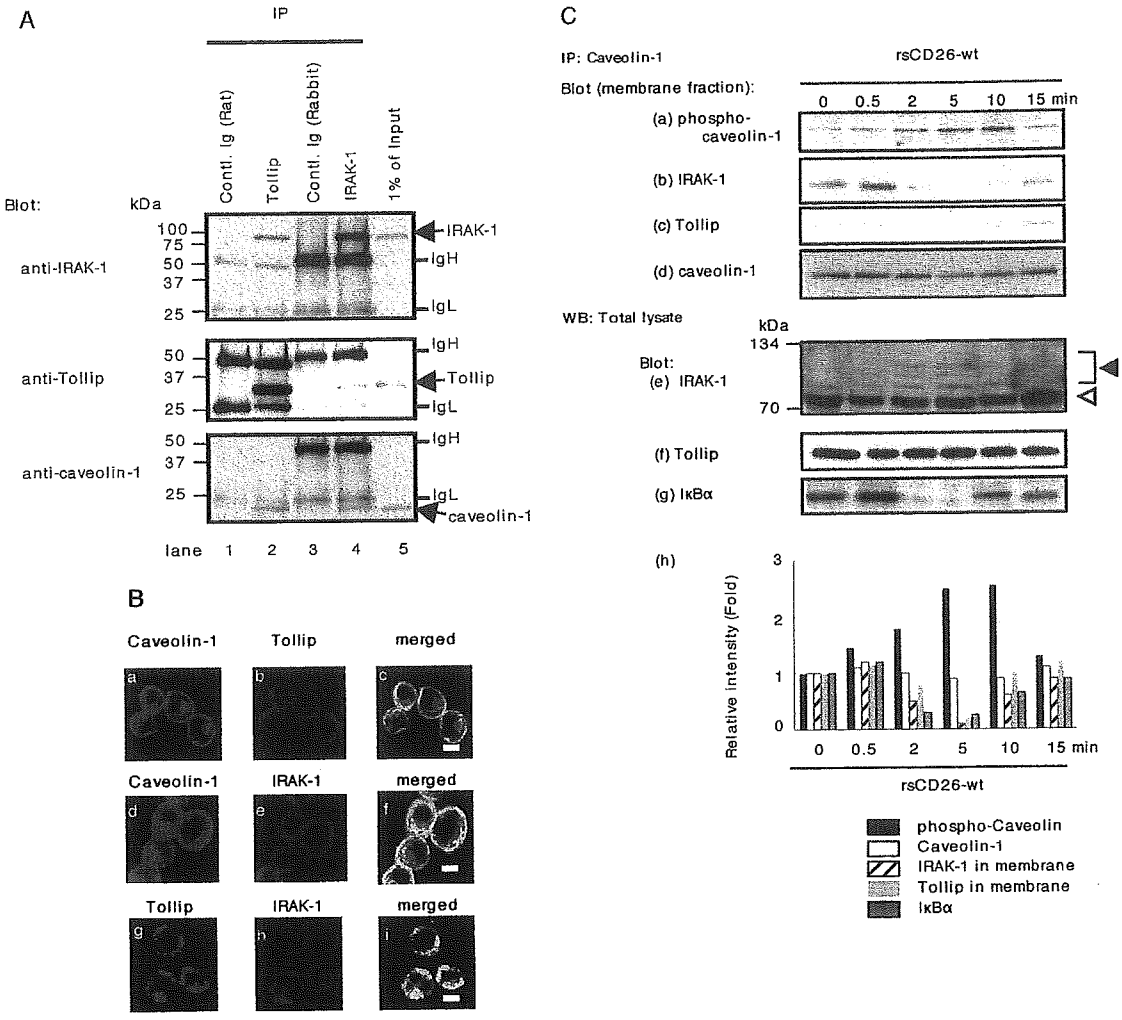

FIG. 2. Caveolin-1 complexes with Tollip and IRAK-1 in monocytes. A. After being pulsed with TT, freshly isolated monocytes were lysed, and IP assays were conducted with anti-Tollip, anti-IRAK-1 antibodies, or control Ig. IP complexes were then separated using 5 to 20% SDS-PAGE followed by Western blotting and were immunoblotted with the indicated antibodies. Shown are the representative results obtained in five independent experiments. IgH and IgL denote immunoglobulin heavy chain and immunoglobulin light chain, respectively. B. TT-loaded monocytes were attached to poly-L-lysine-coated coverslips, fixed with paraformaldehyde, and permeabilized using 0.05% Triton X–PBS. Cells were then stained with anti-caveolin PAb (a and d), anti-Tollip MAb (b and g), or anti-IRAK-1 PAb (e and h), followed by staining with fluorescein isothiocyanate- or Texas red-conjugated secondary antibodies. Cells were visualized by confocal laser microscopy. Observations were made on 50 cells in each of five independent experiments. The micrographs are representative of more than 75% of the cells observed. Bars indicate a 10-μm scale. C. TT-loaded monocytes were stimulated with rsCD26-wt-coated beads for the indicated time periods. Membrane proteins were extracted and immunoprecipitated with anti-caveolin-1 antibody, and immune complexes were resolved by 5 to 20% SDS-PAGE and immunoblotted with anti-phospho-caveolin-1 (a), anti-IRAK-1 (b), or anti-Tollip (c) antibodies, followed by stripping and reprobing with anti-caveolin-1 antibody (d). Total cell lysates from monocytes stimulated as described above were also resolved by 5 to 20% SDS-PAGE and immunoblotted with anti-IRAK (e), anti-Tollip (f), or anti-IκBα (g) antibodies. Position of IRAK-1 bands in e was indicated by an open triangle, and supershifted bands of IRAK-1 were indicated by a solid triangle. The reciprocal intensities of phospho-caveolin-1, caveolin-1, Tollip, and IRAK-1 in membrane proteins that were immunoprecipitated by anti-caveolin-1 were demonstrated (h). The reciprocal intensity of IκBα in total cell lysates was also demonstrated (h). Similar results were obtained in five independent experiments. WB, Western blot.

tagged Tollip mutants were cotransfected into COS cells with HA-tagged caveolin-1–wt (Cav-wt) and VSV-tagged IRAK-1–wt and then precipitated with anti-FLAG MAb. As shown in Fig. 3D, Cav-wt and IRAK-1–wt were coprecipitated with Tollip-wt and Tollip-C2+CUE (lanes 2 and 3). On the other hand, Tollip-ΔCUE and Tollip-C2 coprecipitated only with Cav-wt but not with IRAK-1–wt (lanes 4 and 6), while Tollip-ΔC2 coprecipitated with IRAK-1–wt but not with Cav-wt (lane 5). These data implied that the Tollip C2 domain was required for binding to caveolin-1 and that, as described previously (5), the Tollip CUE domain was required for binding to IRAK-1. Moreover, our findings strongly suggest that caveolin-1 is associated with IRAK-1 and Tollip containing both the C2 and CUE domains. To examine whether caveolin-1 was directly bound to IRAK-1, we next performed IP study with series of HA-tagged caveolin-1 mutants which were cotransfected into COS cells with FLAG-tagged Tollip-wt or Tollip-ΔC2 and VSV-tagged IRAK-1–wt or IRAK-1–ΔCT. As shown in Fig.

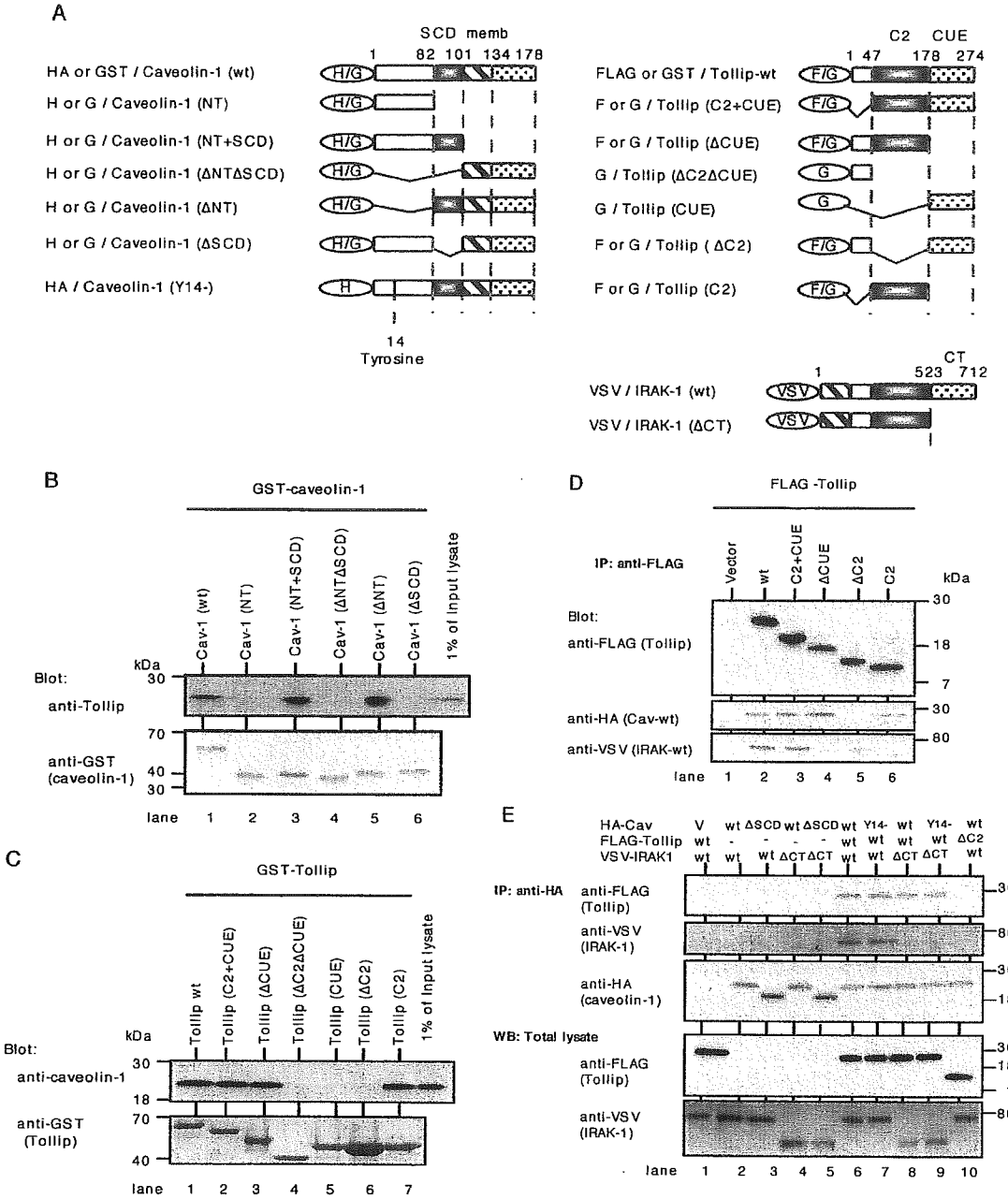

FIG. 3. Determination of the binding domains involved in the interaction among caveolin-1, Tollip, and IRAK-1. A. Schematic representation of HA-tagged or GST-fused caveolin-1, FLAG-tagged or GST-fused Tollip, VSV-tagged IRAK-1, and their mutants. In caveolin-1, residues 1 to 81 comprised the N-terminal region (NT) (open square), residues 82 to 101 comprised the scaffolding domain (SCD) (black square), residues 102 to 134 comprised the transmembrane region (memb; striped square), and residues 135 to 178 comprised the C-terminal region (dotted square). In Tollip, residues 47 to 178 comprised the protein kinase C conserved region 2 (C2 domain) (black square), and residues 179 to 274 comprised coupling of ubiquitin conjugation to endoplasmic reticulum degradation domain (CUE) (dotted square). In IRAK-1, residues 523 to 712 comprised the C-terminal domain (CT) (dotted square). H, G, and F denote HA, GST, and FLAG, respectively. B. GST-fused caveolin-1 and deletion mutants on glutathione-Sepharose (GSH) beads were incubated with THP-1 cell lysate after preclearing with GST on GSH beads. Bound proteins and a 1% amount of input lysate were resolved by 5 to 20% SDS-PAGE and immunoblotted with anti-Tollip MAb, followed by stripping and reprobing with anti-GST MAb. Similar results were obtained in three independent experiments. C. GST-fused Tollip and deletion mutants on GSH beads were incubated with THP-1 cell lysate after preclearing with GST on GSH beads. Bound proteins and a 1% amount of input lysate were resolved by 5 to 20% SDS-PAGE and immunoblotted with anti-caveolin-1 PAb, followed by stripping and reprobing with anti-GST MAb. Similar results were obtained in three independent experiments. D. COS cells were transfected with FLAG-tagged Tollip mutants, HA-tagged caveolin-1–wt, and VSV-tagged IRAK-1–wt, lysed, and immunoprecipitated with anti-FLAG (M2) MAb. Elutions of the FLAG-fusion protein complex were conducted by adding 150 ng/ml of 3× FLAG peptide. The eluted samples were separated using 5 to 20% SDS-PAGE and immunoblotted with anti-HA (caveolin-1–wt) or anti-VSV (IRAK-1–wt) PAbs, followed by stripping and reprobing with anti-FLAG (M2) MAb. Similar results were obtained in three independent experiments. E. COS cells were transfected with HA-tagged caveolin-1, FLAG-tagged Tollip, VSV-tagged IRAK-1, and mutants, lysed, and immunoprecipitated with agarose-conjugated anti-HA MAb. IPs were separated using 5 to 20% SDS-PAGE and immunoblotted with anti-FLAG (M2) (Tollip) MAb or anti-VSV (IRAK-1) PAb, followed by stripping and reprobing with anti-HA (caveolin-1) MAb (top three panels). Whole lysates of COS cells transfected as described above were separated using 5 to 20% SDS-PAGE to resolve expression of transfected FLAG-tagged Tollip and VSV-tagged IRAK-1 and mutants (bottom two panels). Similar results were obtained in three independent experiments. WB, Western blot.

3E, Tollip-wt and IRAK-1–wt were coprecipitated with caveolin-1 (lane 6). On the other hand, IRAK-1 was not coprecipitated with caveolin-1 in the absence of Tollip (lanes 2 to 5), and Cav-wt did not coprecipitate with IRAK-ΔCT even in the presence of Tollip-wt (lane 8). Moreover, Cav-wt did not coprecipitate with Tollip-ΔC2 and IRAK-1–wt (lane 10). Taken together, the above-described results support the notion that the SCD of caveolin-1 binds to the C2 domain of Tollip, the CUE domain of which binds to the C-terminal (CT) domain of IRAK-1. It was observed that caveolin-1 does not bind to IRAK-1 directly.

In the previous study, we showed that caveolin-1 was phosphorylated by CD26 stimulation and transduced signaling events to upregulate CD86 (43). To examine whether phosphorylation of caveolin-1 affected binding to Tollip and IRAK-1, we constructed deletion mutant of tyrosine at residue 14 of caveolin-1 (HA-Cav-Y14)$^-$, and IP study was conducted as described above. As shown in Fig. 3E, the binding capacity of this tyrosine-deleted caveolin-1 to Tollip (lanes 7 and 9) and IRAK-1 (lane 7) did not change compared to that of Cav-wt (lanes 6 and 8). On the other hand, rsCD26-wt was coprecipitated with HA-Cav-Y14, which was not observed to be phosphorylated, while HA-Cav-wt transfected into HEK293 cells was phosphorylated by exogenous rsCD26-wt (data not shown). These results suggest that Cav-Y14 does not affect binding to Tollip and IRAK-1.

Subcellular colocalization of caveolin-1, Tollip, and IRAK-1 in living cells. To confirm the above-described findings in living cells, we performed immunocytochemical analysis with HEK293 cells which were cotransfected with series of caveolin-1, Tollip, and IRAK-1 mutants. GFP-fused or HA-tagged caveolin-1–wt was cotransfected with FLAG-tagged Tollip-wt or Tollip-ΔC2 and VSV-tagged IRAK-1–wt or IRAK-1–ΔCT and stained with anti-FLAG MAb or anti-VSV PAb. As shown in Fig. 4a to c, wild-type proteins of caveolin-1, Tollip, and IRAK-1 were colocalized with each other. On the other hand, caveolin-1–GFP was not colocalized with Tollip-ΔC2 (Fig. 4d) or with IRAK-1–wt in the presence of Tollip-ΔC2 (Fig. 4e), while Tollip-ΔC2 was colocalized with IRAK-1–wt (Fig. 4f). Moreover, following transfection with IRAK-1–ΔCT, caveolin-1–GFP and Tollip-wt were colocalized (Fig. 4g), while IRAK-1–ΔCT was not colocalized with caveolin-1–GFP or with Tollip-wt (Fig. 4h and i). Furthermore, following transfection with Tollip-ΔCUE, caveolin-1–GFP and Tollip-ΔCUE were colocalized, but IRAK-1–wt was not colocalized with caveolin-1–GFP or with Tollip-ΔCUE (data not shown). These data strongly suggest that the SCD of caveolin-1 binds to the C2 domain of Tollip and that the CUE domain of Tollip binds to the CT domain of IRAK-1.

Tollip and IRAK-1 are necessary to enhance human CD86 promoter activity via CD26–caveolin-1 interaction through tyrosine phosphorylation at residue 14 of caveolin-1. In the previous report, we revealed that NF-κB activation downstream of cavelin-1 resulted in the upregulation of CD86 in TT-loaded monocytes stimulated with exogenous CD26 (43). From our present results, we hypothesized that Tollip and IRAK play a role in CD86 upregulation in monocytes downstream of the interaction between CD26 and caveolin-1. To confirm this hypothesis, we evaluated CD86 promoter activity following the interaction between CD26 and caveolin-1 in the

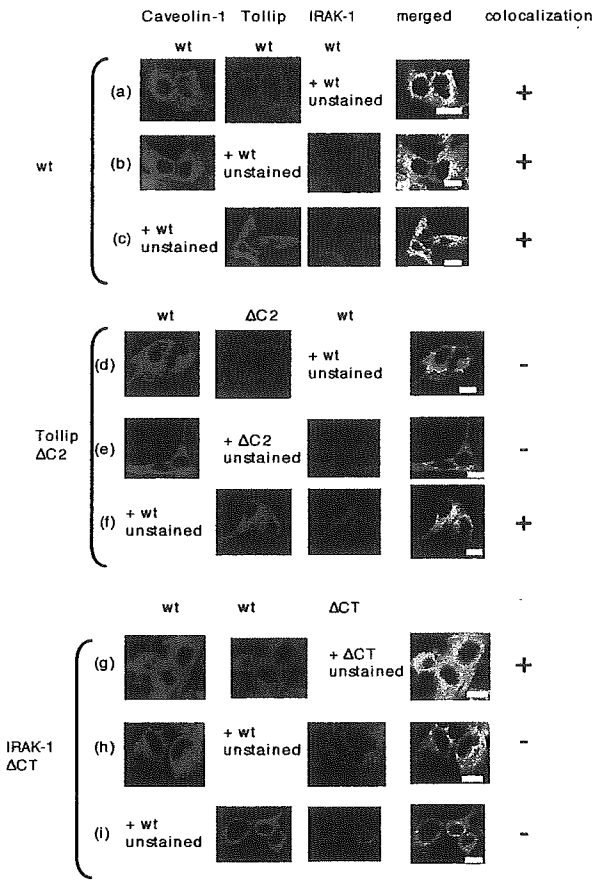

FIG. 4. Subcellular colocalization of caveolin-1, Tollip, and IRAK-1 in living cells. HEK293FT cells were transfected with GFP-fused (a, b, d, e, g, and h) or HA-tagged (c, f, and i) caveolin-1-wt, FLAG-tagged Tollip (wt or ΔC2), and VSV-tagged IRAK-1 (wt or ΔCT). Cells were then fixed and permeabilized with acetone-methanol and stained with anti-FLAG (M2) MAb or anti-VSV PAb, followed by staining with anti-mouse Ig (fluorescein isothiocyanate- or Texas red-conjugated) or anti-rabbit Ig (Texas red-conjugated) antibodies. Stained cells were mounted using a Prolong Antifade kit. Observations were made with 10 to 15 cells in each of five different experiments. The micrographs are representative of more than 75% of the cells observed. Bars indicate a 10-μm scale.

presence or absence of Tollip and IRAK-1 by using luciferase chimera of the 5′-flanking promoter region of human CD86 (a 1.3-kb fragment upstream of the transcriptional site of the CD86 gene), which was described previously (43). CD86 promoter activity was enhanced following cotransfection of Tollip-wt in a dose-dependent manner in the presence of caveolin-1–wt (Fig. 5A, top). However, CD86 promoter activity was not detected in the presence of Tollip-ΔC2 or Tollip-ΔCUE with caveolin-1–wt or caveolin-1 Y14 (Fig. 5A, top). Moreover, increasing doses of IRAK-1–wt resulted in increased activity of the CD86 promoter with caveolin-1–wt but not with caveolin-1 Y14 (Fig. 5B, top). Moreover, CD86 promoter activity was not detected in the presence of IRAK-ΔCT with caveolin-1–wt or caveolin-1 Y14 (Fig. 5B, top). On the other hand, activation of the CD86 promoter was not observed by stimulation with CD26 lacking the CBD (CD26-Δ201) or with medium alone (middle and bottom panels of Fig. 5A and

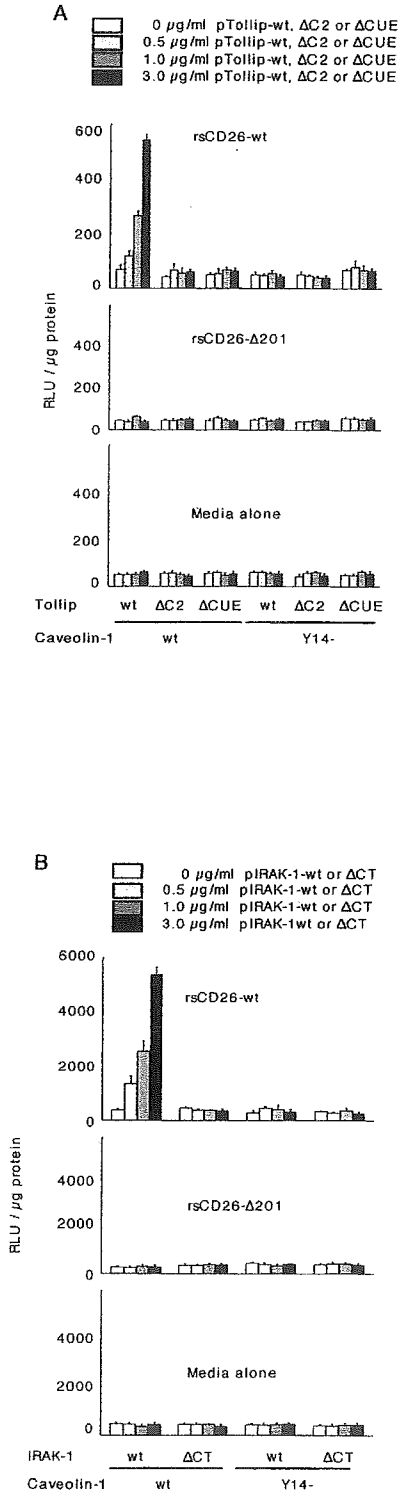

FIG. 5. Enhanced CD86 promoter activity by increasing doses of Tollip or IRAK-1 in response to exogenous CD26 stimulation. A. Twelve hours after HEK293 cells were cotransfected with human CD86-promoter luciferase constructs, caveolin-1 (wt or deleting tyrosine at residue 14 mutant [Y14$^-$]) and Tollip (wt, ΔC2, or ΔCUE) vectors, wild-type-soluble CD26 (rsCD26-wt), or rsCD26 lacking the caveolin-binding domain (rsCD26-Δ201) was added to the culture medium and incubated for an additional 20 h. Cells were harvested for measurement of luciferase activity and protein concentration. Luciferase activity is shown as being relative to 1 μg of applied protein. Data represent means ± standard errors (SE) from triplicate experiments. B. HEK293 cells were cotransfected with human CD86-promoter luciferase constructs, caveolin-1 (wt or Y14$^-$), and IRAK-1 (wt or ΔCT) vectors, treated, and prepared for luciferase assay as described above. RLU, relative light units.

B). These data strongly suggest that tyrosine phosphorylation of caveolin-1 at residue 14 is necessary to induce activation of NF-κB to upregulate CD86 expression via Tollip and IRAK-1 following CD26–caveolin-1 interaction.

siRNA against Tollip attenuates CD26-mediated upregulation of CD86 and inhibits T-cell proliferation driven by tetanus toxoid. To examine CD26–caveolin-1–Tollip interaction on TT-mediated T-cell proliferation more directly, we performed siRNA experiments in freshly isolated monocytes. For this purpose, we prepared two sets of specific siRNAs against Tollip as described in Materials and Methods, and both of these siRNAs decreased Tollip expression in monocytes (Fig. 6A, lanes 3 and 4). Since Tollip expression in monocytes was not significantly affected by HVJ-E vector or mismatched siRNA (lanes 2 and 5), this inhibitory effect by siRNA was specific. siRNA or HVJ-E vector did not affect expression levels of IRAK-1 and caveolin-1 (Fig. 6A). We next examined whether exogenously added CD26 exerted its effect on monocytes in which Tollip expression was attenuated by siRNA. For this purpose, freshly isolated monocytes that were untreated or treated with siRNA against Tollip were incubated with rsCD26-wt or CD26-Δ201 beads in the presence or absence of TT, and the expression of CD86 on monocytes was examined using flow cytometric analysis. As shown in Fig. 6B, CD86 expression on monocytes with medium alone or mis-siRNA treatment was increased significantly after TT and rsCD26-wt stimulation (Fig. 6B) as reported previously (42, 43). This enhancing effect was not observed following treatment with rsCD26-Δ201 beads, which did not stimulate caveolin-1 on monocytes (Fig. 6B). On the other hand, treatment with siRNA against Tollip in monocytes resulted in a significant decrease in CD86 expression when monocytes were pulsed with TT and rsCD26-wt beads (Fig. 6B). In fact, the CD86 expression level in these monocytes (Fig. 6B) was similar to the level seen in monocytes that were not treated other than with TT plus rsCD26-wt (Fig. 6B). These results suggest that Tollip plays an important role in signal transduction following CD26 binding to TT-loaded monocytes, leading to the upregulation of CD86, as shown in our previous study using monocytes of caveolin-1 knockdown (43).

In the previous study, we demonstrated that activation of NF-κB was involved in upregulation of CD86 following CD26–caveolin-1 interaction (43). In Fig. 1 and 2, we showed that Tollip mediates activation of NF-κB via phosphorylation of caveolin-1 by exogenous CD26. To elucidate the more direct effect of Tollip on inducing activation of NF-κB, we examined activation of NF-κB using an ELISA-based DNA-binding detection method. As shown in Fig. 6C, We detected significant levels of the p50 and p65 NF-κB components in nuclear extracts (NE) of TT-loaded monocytes stimulated with wild-type CD26 (Fig. 6C). The increase in p50 and p65 NF-κB levels was inhibited by treatment of siRNA against Tollip (Fig. 6C). On

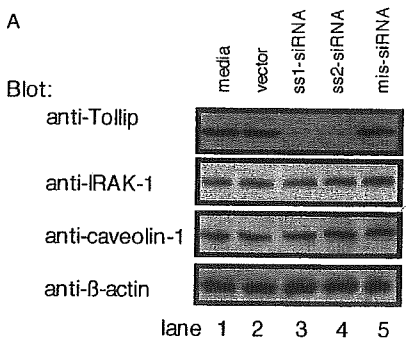
A
media
vector
ss1-siRNA
ss2-siRNA
mis-siRNA
Blot:
anti-Tollip
anti-IRAK-1
anti-caveolin-1
anti-ß-actin
lane 1 2 3 4 5

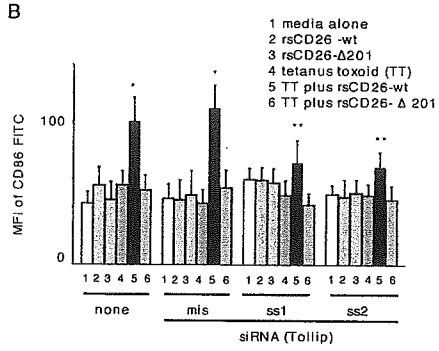
B
1 media alone
2 rsCD26 -wt
3 rsCD26-Δ201
4 tetanus toxoid (TT)
5 TT plus rsCD26-wt
6 TT plus rsCD26- Δ 201
MFI of CD86 FITC
100
0
1 2 3 4 5 6 1 2 3 4 5 6 1 2 3 4 5 6 1 2 3 4 5 6
none
mis
ss1
ss2
siRNA (Tollip)

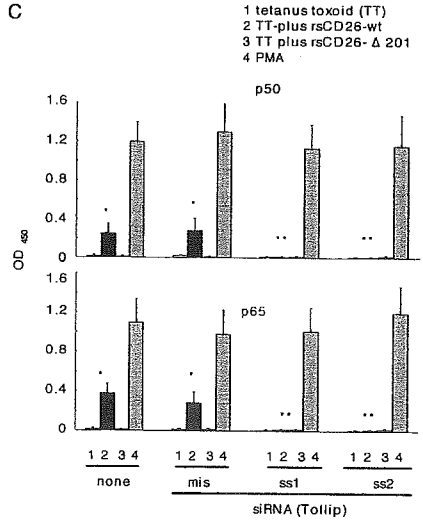
C
1 tetanus toxoid (TT)
2 TT-plus rsCD26-wt
3 TT plus rsCD26- Δ 201
4 PMA
p50
p65
OD 450
1.6
1.2
0.8
0.4
0
1 2 3 4 1 2 3 4 1 2 3 4 1 2 3 4
none
mis
ss1
ss2
siRNA (Tollip)

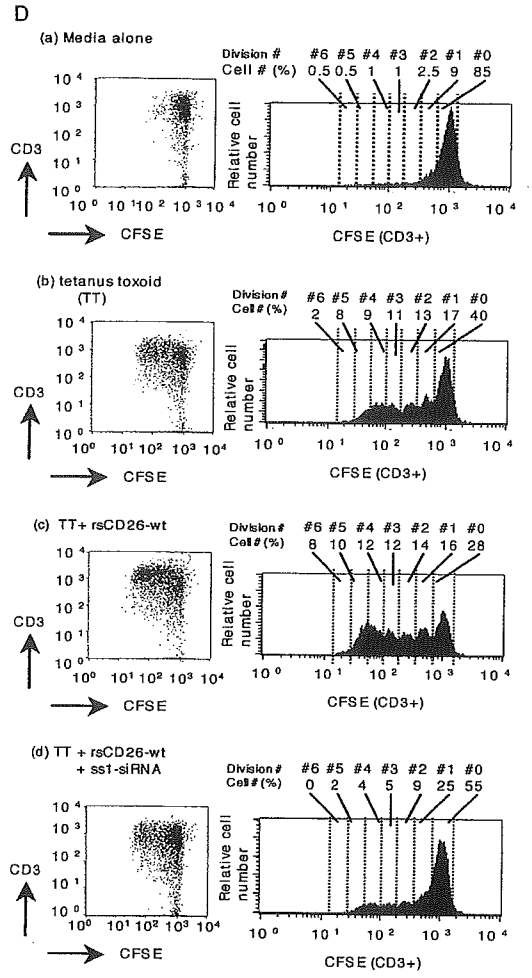
D
(a) Media alone
Division # #6 #5 #4 #3 #2 #1 #0
Cell # (%) 0.5 0.5 1 1 2.5 9 85
CD3
CFSE
Relative cell number
CFSE (CD3+)
(b) tetanus toxoid (TT)
Division # #6 #5 #4 #3 #2 #1 #0
Cell # (%) 2 8 9 11 13 17 40
(c) TT+ rsCD26-wt
Division # #6 #5 #4 #3 #2 #1 #0
Cell # (%) 8 10 12 12 14 16 28
(d) TT + rsCD26-wt + ss1-siRNA
Division # #6 #5 #4 #3 #2 #1 #0
Cell # (%) 0 2 4 5 9 25 55

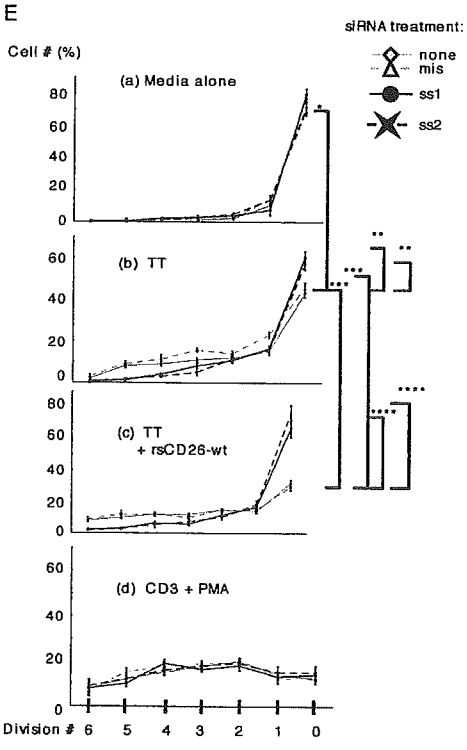
E
siRNA treatment:
none
mis
ss1
ss2
Cell # (%)
(a) Media alone
(b) TT
(c) TT + rsCD26-wt
(d) CD3 + PMA
Division # 6 5 4 3 2 1 0

the other hand, the levels of p50 and p65 NF-κB did not alter in NE of TT-loaded monocytes stimulated with TT alone or with CD26 lacking the CBD (CD26-Δ201) (Fig. 6C), and siRNA treatment did not alter activation of p50 and p65 by PMA (Fig. 6C). These results strongly suggest that Tollip plays an important role in signal transduction to activate of NF-κB following CD26 binding to TT-loaded monocytes, leading to the upregulation of CD86, as shown in our previous study using caveolin-1 knockdown monocytes (43).

Furthermore, to determine whether T-cell proliferation pulsed with TT was inhibited in the presence of monocytes with decreased Tollip expression, proliferation assays were performed using CFSE as described in Materials and Methods, with purified T cells being from the same donor as the prepared monocytes. In studies involving the CFSE fluorescent profile, TT-induced T-cell proliferation was observed in the presence of monocytes with unaffected Tollip levels (Fig. 6D, panels a and b), as demonstrated by the increased numbers of CFSE fluorescence intensity of $CD3^+$ cells. Meanwhile, TT-induced T-cell proliferation was significantly enhanced in the presence of exogenous rsCD26 (Fig. 6D, panel c), as described previously (42, 43, 57). This effect was clearly inhibited by Tollip knockdown (Fig. 6D, panel d). To quantify these observations, cell numbers to each cell division number determined by CFSE fluorescence intensity of $CD3^+$ subset with or without various treatments were demonstrated in line graphs (Fig. 6E). TT-induced T-cell proliferation was observed without Tollip knockdown (Fig. 6E), and this proliferation was significantly inhibited by Tollip knockdown in monocytes (Fig. 6E). On the other hand, as described previously (42, 43, 57), TT-induced T-cell proliferation was significantly enhanced in the presence of exogenous rsCD26 (Fig. 6E). This effect was more profoundly suppressed by Tollip knockdown than the inhibition observed with TT alone (Fig. 6E). Knockdown of Tollip in monocytes did not have an effect on anti-CD3 plus PMA-stimulated T-cell proliferation (Fig. 6E, panel d). Moreover, rsCD26-Δ201 did not enhance TT-mediated T-cell proliferation (data not shown). These results demonstrate that Tollip has an important role in the enhancement of TT-induced T-cell proliferation following treatment with exogenous CD26.

siRNA against IRAK-1 attenuates CD26-mediated upregulation of CD86 and inhibits T-cell proliferation driven by tetanus toxoid. To examine directly the role of IRAK-1 in caveolin-1-induced CD86 activation, we performed siRNA experiments in freshly isolated monocytes. ss3-siRNA, designed for knockdown of human IRAK-1, decreased IRAK-1 expression in monocytes (Fig. 7A, lanes 3). We examined whether exogenously added CD26 exerted its effect on monocytes in which IRAK-1 expression was attenuated by ss3-siRNA. For this purpose, freshly isolated monocytes that were untreated or treated with siRNA against IRAK-1 were incubated with rsCD26-wt or rsCD26-Δ201 beads in the presence or absence of TT, and the expression of CD86 on monocytes was examined using flow cytometric analysis. As shown in Fig. 7B, CD86 expression on monocytes treated with medium alone or mis-siRNA was increased significantly after TT and rsCD26-wt stimulation, as reported previously (42, 43) and as observed in Fig. 6B. This enhancing effect was not observed following treatment with rsCD26-Δ201 beads, which did not stimulate caveolin-1 on monocytes (Fig. 7B). On the other hand, treatment with siRNA against IRAK-1 in monocytes resulted in a significant decrease in CD86 expression when monocytes were pulsed with TT and rsCD26-wt beads (Fig. 7B). In fact, the CD86 expression level in these monocytes (Fig. 7B) was similar to the level seen in monocytes treated with stimuli other than rsCD26-wt plus TT (Fig. 7B). These results suggest that IRAK-1 also plays an important role in signal transduction following CD26 binding to TT-loaded monocytes, leading to the upregulation of CD86, as shown in our previous study using Tollip (Fig. 6B) or caveolin-1 knockdown monocytes (43).

Moreover, we detected significant levels of the p50 and p65

FIG. 6. siRNAs against Tollip inhibit the effect of exogenous CD26 on CD86 upregulation in TT-loaded monocytes and proliferation of T cells in response to TT. A. Purified monocytes were transfected with or without sense siRNA (ss1 is targeted for positions +186 to +206, and ss2 is targeted for positions +774 to +794) of the Tollip gene or mismatched siRNA (mis-siRNA) by using the HVJ-E vector. Cell lysates were resolved by 5 to 20% SDS-PAGE and immunoblotted with the indicated antibodies, followed by stripping and reprobing with anti-β-actin antibody. All experiments were performed at least five times with similar results. B. Purified monocytes were transfected with or without siRNA using the HVJ-E vector, followed by treatment with TT. After stimulation with rsCD26 (wt or Δ201)-coated beads, cells were subjected to analysis of surface CD86 expression by flow cytometry. Monocytes were identified by gating of the CD45-Cy Chrome- and CD14-phycoerythrin-positive population. Mean fluorescence intensity (MFI) of cell surface CD86 is demonstrated. Data represent means ± SE of five independent experiments. * shows points of significant increase ($P < 0.05$), whereas ** indicates points of no significant change compared to controls. FITC, fluorescein isothiocyanate. C. TT-loaded monocytes with or without siRNA treatment were stimulated with CD26-coated beads and harvested for extraction of nuclear proteins (NE). Each 5 μg of NE was subjected to an ELISA-based DNA-binding protein assay. Binding activity to p50 and p65 NF-κB components was revealed by an optical density value at 450 nm (OD_{450}). Data represent means ± SE from triplicate experiments. * shows points of significant increase ($P < 0.05$), whereas ** indicates points of no significant change compared to controls. D. Kinetic analyses of T-cell division as proliferation in populations of CFSE-labeled T cells. Isolated T cells were labeled with CFSE and cultured for 96 h with monocytes isolated from the same donor. T cells were cocultured with untreated monocytes (a), with TT-loaded monocytes (b), with TT-loaded monocytes followed by addition of rsCD26-wt (c), and with siRNA ss1-treated monocytes pulsed with TT and rsCD26-wt (d). T cells were revealed by $CD3^+$ populations in dot plots as shown in the left panels. Histograms of the right panels show the CFSE fluorescence profile of $CD3^+$ subsets from each dot gram. The numbers appearing above each histogram denote each division population (upper "Division #") and percent cell numbers in each division [lower "Cell # (%)"]. The undivided T cells reside in the rightmost peak, and the T cells having divided six times reside in the leftmost peak. The experiment depicted here is representative of five separate experiments. E. Kinetic analyses of T-cell division as proliferation in populations of CFSE-labeled T cells were shown as sequential line graphs, conducted as described above (C). T cells were cocultured with untreated monocytes (a), with TT-loaded monocytes (b), with TT-loaded monocytes followed by addition of rsCD26-wt (c), and in the presence of soluble anti-CD3 plus PMA (d). Before coculture with T cells, monocytes were treated with or without siRNAs as described in Materials and Methods. The numbers appearing under each graph denote each division population (Division #), and the verticals are the percent cell numbers in each division [Cell # (%)]. Data represent means ± SE from triplicate experiments. Asterisks depict significant changes ($P < 0.05$).

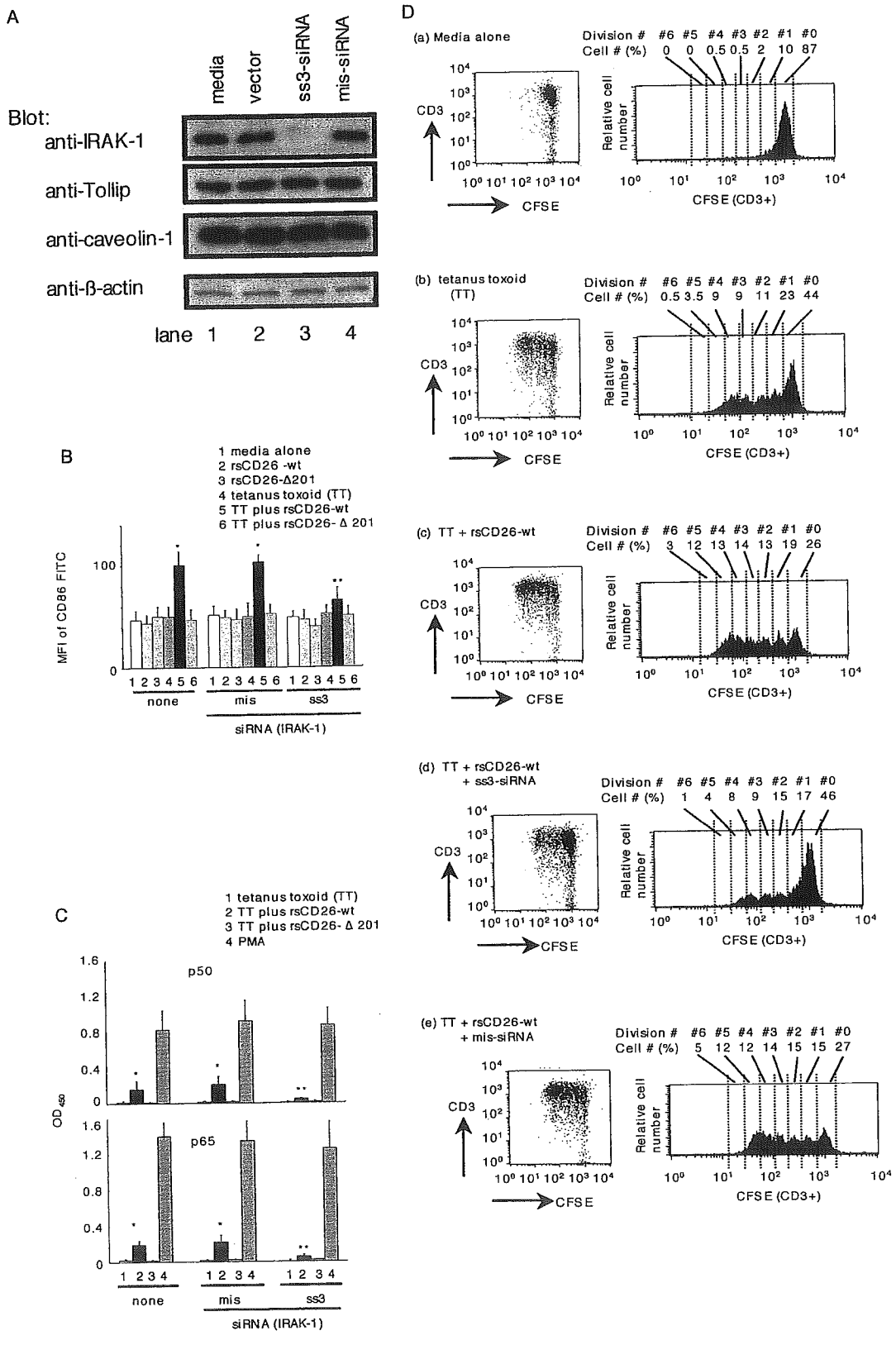

FIG. 7. siRNAs against IRAK-1 inhibit the effect of exogenous CD26 on CD86 upregulation in TT-loaded monocytes and proliferation of T cells in response to TT. A. Purified monocytes were transfected with or without ss3-siRNA (targeted for positions +969 to +989 of human IRAK-1 gene) or mismatched siRNA (mis-siRNA) by using the HVJ-E vector. Cell lysates were resolved by 5 to 20% SDS-PAGE and immunoblotted with the indicated antibodies, followed by stripping and reprobing with anti-β-actin antibody. All experiments were performed at least five times with

NF-κB components in NE of TT-loaded monocytes stimulated with wild-type CD26 (Fig. 7C), and the increase in p50 and p65 NF-κB levels was inhibited by treatment of siRNA against IRAK-1 (Fig. 7C). On the other hand, the levels of p50 and p65 NF-κB did not alter in NE of TT-loaded monocytes stimulated with TT alone or with CD26 lacking the CBD (CD26-Δ201), and siRNA treatment did not affect activation of p50 or p65 by PMA (Fig. 7C). These results strongly suggest that IRAK-1 also plays an important role in signal transduction to activate NF-κB following CD26 binding to TT-loaded monocytes, leading to the upregulation of CD86, as shown in Fig. 6 using siRNA against Tollip and as observed in our previous study using caveolin-1 knockdown monocytes (43).

Finally, to determine whether T-cell proliferation pulsed with TT was inhibited in the presence of monocytes with decreased IRAK-1 expression, proliferation assays were performed using CFSE, similar to the methods used for the studies described in the legend of Fig. 6D and E. In studies involving the CFSE fluorescent profile, TT-induced T-cell proliferation was observed in the presence of monocytes with unaffected IRAK-1 levels (Fig. 7D, panels a and b). Despite the fact that TT-induced T-cell proliferation was significantly enhanced in the presence of exogenous rsCD26 (Fig. 7D, panel c), this effect was clearly inhibited by IRAK-1 knockdown (Fig. 7D, panel d). Mismatched siRNA (mis-siRNA) did not alter enhancement of exogenous CD26-mediated T-cell proliferation, and knockdown of IRAK-1 in monocytes did not have an effect on anti-CD3 plus PMA-stimulated T-cell proliferation (data not shown). These results demonstrate that IRAK-1 has an important role in the enhancement of TT-induced T-cell proliferation following treatment with exogenous CD26.

DISCUSSION

In the previous study, we identified caveolin-1 in APC as a binding protein for CD26 and demonstrated that external CD26 stimulation induced phosphorylation of caveolin-1 to enhance surface expression of CD86 on APC by activation of NF-κB (43). This interaction resulted in enhancing CD26-mediated T-cell proliferation in response to recall antigen such as TT (42, 43). However, it remains to be elucidated as to how caveolin-1 is linked to the activation of NF-κB in monocytes.

In the present study, we demonstrated that caveolin-1 binds to Tollip and IRAK-1 in the membrane of TT-loaded monocytes and that following exogenous CD26 stimulation, Tollip and IRAK-1 disengage from caveolin-1, with IRAK-1 being subsequently phosphorylated to upregulate CD86 expression. Moreover, we showed that Tollip plays an important role in the interaction among caveolin-1, Tollip, and IRAK-1 and in CD26–caveolin-1 signaling to upregulate CD86, resulting in subsequent T-cell proliferation in response to TT.

To identify the proteins associated with caveolin-1 following exogenous CD26 stimulation, we conducted proteomic analysis of TT-loaded monocytes in the presence or absence of exogenous CD26 stimulation and identified a decrease in the level of Tollip and IRAK-1 among membrane proteins following CD26-wt stimulation (Fig. 1). It was previously reported that Tollip was involved in IL-1R/Toll-like receptor (TLR)-mediated signaling and that it linked IRAK to NF-κB, Jun N-terminal protein kinase, and p38 mitogen-activated protein kinase (7, 10). Originally, Tollip was cloned as a protein that interacts with the IL-1R accessory protein (5). Subsequently, Tollip was shown to associate directly with the cytoplasmic TIR domains of IL-1Rs, TLR2, and TLR4 following the stimulation of these receptors and to inhibit TLR-mediated cellular responses by suppressing the phosphorylation and kinase activity of IRAK-1 (62). In resting cells, Tollip forms a complex with members of the IRAK family, thereby preventing NF-κB activation by blocking the phosphorylation of IRAK-1. After receptor activation, Tollip–IRAK-1 complexes are recruited to the IL-1Rs TLR2 and TLR4, which results in the rapid autophosphorylation of IRAK-1 and its dissociation from the receptors. At the same time, IRAK-1 phosphorylates Tollip, which might then lead to the dissociation of Tollip from IRAK-1 and to its rapid ubiquitylation and degradation (25, 50). Tollip is therefore thought to function mainly to maintain immune cells in a quiescent state and to facilitate the termination of IL-1R/TLR-induced cell signaling during inflammation and infection. However, our present findings showed that Tollip in TT-loaded monocytes functioned as a recruiter of IRAK-1 to caveolin-1 after CD26-mediated phosphorylation of caveolin-1 and then transduced intracellular signals to activate NF-κB, leading to the upregulation of CD86 expression (Fig. 2C, 5A and B, and 6B to D). Moreover, other investigators reported that increased expression of Tollip was observed after LPS challenge, and thus, hyporesponsiveness to LPS was prolonged with Tollip serving as a suppressor (1, 30). However, we observed that the total expression level of Tollip did not change following exogenous CD26 stimulation and dissocia-

similar results. B. Purified monocytes were transfected with or without siRNA using the HVJ-E vector, followed by treatment with TT. After stimulation with rsCD26 (wt or Δ201)-coated beads, cells were subjected to analysis of surface CD86 expression by flow cytometry with the same method as described in the legend of Fig. 6B. Mean fluorescence intensity (MFI) of cell surface CD86 is demonstrated. Data represent means ± SE of five independent experiments. * shows points of significant increase ($P < 0.05$), whereas ** indicates points of no significant change compared to controls. FITC, fluorescein isothiocyanate. C. TT-loaded monocytes with or without siRNA treatment were stimulated with CD26-coated beads and harvested for extraction of nuclear proteins (NE). Each 5 μg of NE was subjected to an ELISA-based DNA-binding protein assay as described in the legend of Fig. 6C. Data represent means ± SE from triplicate experiments. * shows points of significant increase ($P < 0.05$), whereas ** indicates points of no significant change compared to controls. OD_{450}, optical density at 450 nm. D. Kinetic analyses of T-cell division as proliferation in populations of CFSE-labeled T cells using the same method as described in the legend of Fig. 6D. T cells were cocultured with untreated monocytes (a), with TT-loaded monocytes (b), with TT-loaded monocytes followed by addition of rsCD26-wt (c), and with ss3-siRNA-treated (d) or mis-siRNA-treated (e) monocytes pulsed with TT following rsCD26-wt stimulation. T cells were revealed by $CD3^+$ populations in dot plots as shown in the left panels. Histograms of the right panels show the CFSE fluorescence profile of $CD3^+$ subsets from each dot plot. The numbers appearing above each histogram denote each division population (upper "Division #") and percent cell numbers in each division [lower "Cell # (%)"]. The undivided T cells reside in the rightmost peak, and the T cells having divided six times reside in the leftmost peak. The experiment depicted here is representative of five separate experiments.

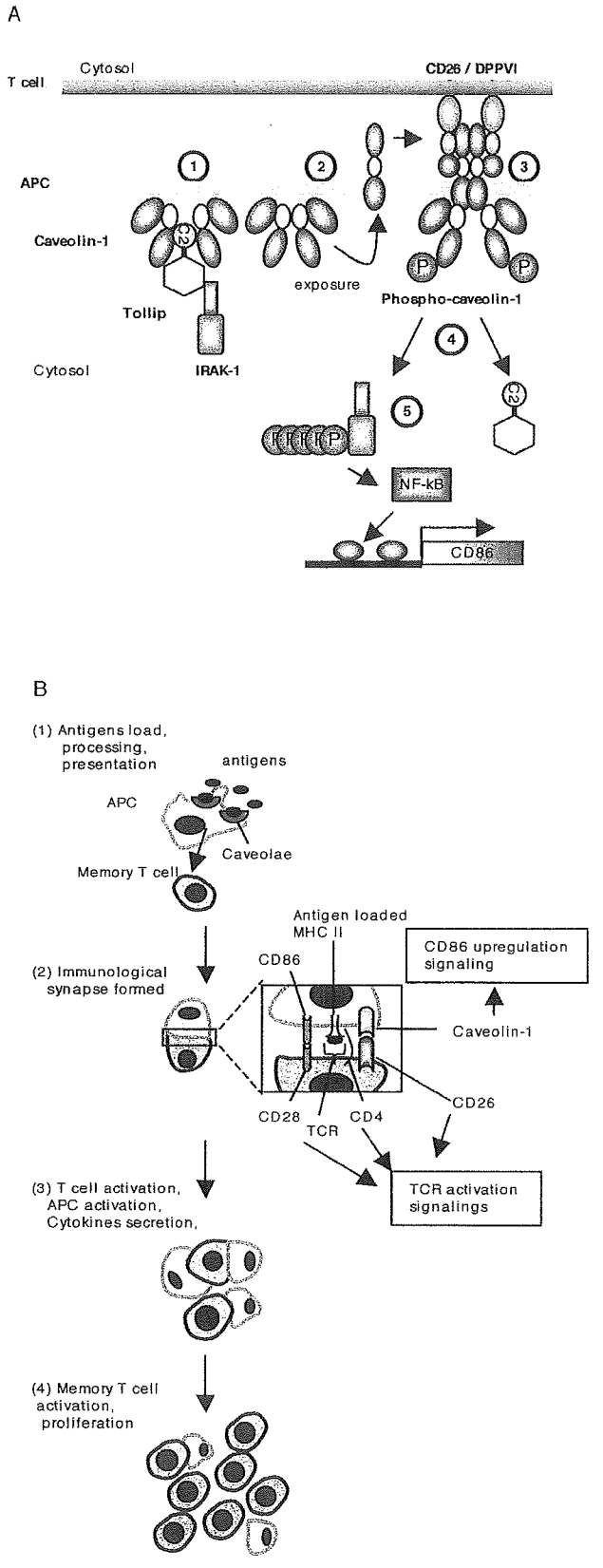

FIG. 8. Model for CD26–caveolin-1 interaction leading to upregulation of CD86. A. Caveolin-1 in monocytes (APC) resides at the inner membrane in the presence or absence of Tollip and IRAK-1 (1). After uptake of tetanus toxoid into monocytes via caveolae, some population of caveolin-1 is exposed on the outer cell surface of TT-loaded monocytes (2). Migration of $CD26^+$ antigen-specific memory T cells to areas of antigen-loaded APCs results in contact with TT APC, leading to the association of CD26 and caveolin-1 (3). Aggregation of caveolin-1 in the contact area occurs, presumably by homo-oligomerization (via its residues 61 to 101), followed by its phosphorylation. Phosphorylated caveolin-1 (phospho-caveolin-1) dissociates complexed Tollip and IRAK-1, presumably due to conformational changes, and IRAK-1 is then phosphorylated in the cytosol (4). After IRAK is phosphorylated, NF-κB is activated to lead to upregulation of CD86 (5). B. Antigens such as tetanus toxoid are loaded into monocytes and are then processed and presented with MHC class II (MHC II) on the cell surface along with exposure of caveolin-1 N terminus (1). Memory T cells expressing CD26 have contact with these antigen-presenting cells, and maturation of the immunological synapse occurs via T-cell receptor (TCR)-MHC class II, CD28-CD86/CD80, and CD26–caveolin-1 interactions (2). T cells and APC are then activated and cytokines are secreted (3). CD86 upregulation therefore leads to greater T-cell–APC interaction and the development of activated T cells locally and activated immune response, resulting in potential autoimmune diseases (4).

tion from caveolin-1, although the Tollip level in the cell membrane was decreased (Fig. 2C, panels c and f). Although the precise mechanism is not known, we speculate that a change in the total level of Tollip was not observed since only a small amount of membrane Tollip exists in comparison to excess level of Tollip in the cytoplasm (Fig. 2A and B). Although IRAK-M is a catalytically inactive kinase in monocytes that suppresses IRAK-1 function by inhibiting phosphorylation of IRAK-1 or preventing its dissociation from the receptor complex (26), we did not observe an association between caveolin-1 and IRAK-M (data not shown).

The generation of IRAK-1 knockout mice has revealed an important role for this kinase in signaling by TLR4 as well as the IL-1R (24, 53, 59). Cells lacking IRAK-1 exhibit an impaired ability to activate p38 mitogen-activated protein kinase, Jun N-terminal protein kinase, and NF-κB and to secrete inflammatory cytokines (e.g., tumor necrosis factor alpha [TNF-α] and IL-6) when stimulated with LPS or IL-1 (24, 53, 59). Notably, IRAK-1-deficient mice are less susceptible to the lethal effects of LPS than their wild-type counterparts (53). Despite this, whether IRAK-1 plays a role in immune response of memory T cells has not been described, presumably because there are many differences in adoptive immunity between mice and humans (36). In particular, $CD26^+$ T cells have different functions in mice and humans. In mice, the CD26 molecule was found as a thymocyte-activating molecule expressed on CD4 CD8 double-negative immature thymocytes, and this molecule might be involved in an important activation pathway during thymocyte differentiation (41). On the other hand, CD26 was originally characterized as a T-cell activation antigen in human T cells and expressed on $CD4^+$ or $CD8^+$ medullary thymocytes in the human thymus (39). Human CD26 is also preferentially expressed on a specific population of T lymphocytes, the subset of $CD4^+$ memory T cells, and is upregulated after T-cell activation (11, 12, 38). Thus, the murine system may not be appropriate for studying CD26 and adoptive immunity, especially compared to the human system.

Our findings, which establish a biochemical protein-protein association, raise questions about the functional implication of

caveolin-1 binding to Tollip and IRAK-1 as well as exogenous CD26. Many other receptor systems appear to localize to caveoli, which are defined by their cholesterol- and sphingomyelin-enriched lipid environments as well as by their morphological features (51). As an example, TNF receptor (TNFR)-associated factor 2 (TRAF2) is reported to be associated with caveolin-1 to activate NF-κB signaling by clustering caveolin-1–TRAF2 and TNFR2 (15). If exogenous CD26 were associated with caveolin-1 and TRAF2 clustering, 2D-PAGE analysis of membrane proteins of APC may detect changes in the levels of other proteins. However, we only observed changes in the levels of Tollip and IRAK-1, as shown in Fig. 1. Further study will be needed to determine whether caveolin-1–CD26 association alters signaling complexes other than Tollip and IRAK-1. Another issue raised by our findings is how the complex containing exogenous CD26 and caveolin-1 clusters with the complex containing Tollip and caveolin-1, since both CD26 and Tollip bind to the SCD of caveolin-1 (Fig. 3B and our previous report [43]). Our speculation is as follows: a part of caveolin-1 binds to Tollip in the cytoplasm, while another part of caveolin-1 binds to exogenous CD26 following the external exposure of caveolin-1 that accompanies processing of TT. Both heterocomplexes may associate with each other via interaction of the homo-oligomerization domain (residues 61 to 101) of caveolin-1 (49, 52). It would be of considerable interest to define this interaction in future studies. Degradation of IRAK-1 after CD26–caveolin-1 stimulation is another issue to be elucidated. It has been reported that specific phosphorylated amino acids on IRAK-1 contributed to recognition by ubiquitin ligases, which mark phosphorylated IRAK-1 for proteasomal degradation (6, 31, 60). On the other hand, other investigators suggested that IRAK-1 is not degraded but is instead translocated to the nucleus upon IL-1 treatment, where it fulfills an unidentified function (3). Although the exact role of IRAK-1 degradation in IL-1 signaling is controversial, it is known that degradation of IRAK-1 leads to a shutdown of the IL-1 response and represents a negative feedback loop in the NF-κB pathway. So far, the precise mechanism of IRAK-1 ubiquitination and degradation has not been studied, but Tollip is a good candidate to bring the ubiquitination machinery into the proximity of IRAK-1 (25, 62). It is important to elucidate the metabolic pathways of IRAK-1 as well as Tollip following CD26-mediated caveolin-1 phosphorylation in future studies.

On the basis of our results and previously reported findings, we propose a model to describe the signaling events in monocytes triggered by CD26–caveolin-1 interaction (Fig. 8A). In this model, a part of N termini of caveolin-1 is exposed after tetanus toxoid is trafficked in monocytes (43), and CD26 induces aggregation and phosphorylation of caveolin-1 expressed in the T-cell–APC contact area as demonstrated in our previous report (43). Following caveolin-1 phosphorylation, dissociation of Tollip and IRAK-1 is induced with subsequent phosphorylation of IRAK in the cytosol. This sequence of events allows for activation of NF-κB and transcription of the CD86 gene. T cells then expand clonally and acquire additional effector functions as a result of CD26–caveolin-1 interaction as well as CD28-B7 and CD40-CD154 interaction (2, 29, 35). Consequently, T-cell proliferation that is dependent on the presence of CD26 is observed in response to recall antigen such as tetanus toxoid (Fig. 8B).

In endothelial cells (EC), inhibition of the scaffolding domain of caveolin-1 reduces inflammation by inhibition of endothelial nitric oxide synthetase, which is bound to caveolin-1 (4). Moreover, human EC in vivo express constitutively major histocompatibility (MHC) class II molecules and caveolin-1 (9, 51), whereas murine EC do not express MHC class II molecules (9). Thus, human EC have an ability to present antigens to $CD4^+$ T cells inducing proliferation of memory T cells (46) and play an important role in grafting of transplants (54) as well as in presenting recall antigens in human delayed hypersensitivity reactions (13, 46). In this regard, inhibition of caveolin-1 and CD26 interaction in the human system may provide a significant treatment strategy not only for the inflammatory state but also for transplantation. In the clinical setting, patients with autoimmune diseases such Graves' disease and rheumatoid arthritis have increased levels of $CD26^+$ T cells in inflamed tissues such as thyroid and synovial membrane and fluids (14, 37). In addition, enhancement of CD26 expression in these autoimmune diseases may correlate with disease severity (17, 40). Moreover, it has been shown that T cells migrating through endothelial cell monolayers in vitro express high levels of CD26 (33, 34), while the fact that chemokines play a key role in T-cell migration supports the notion that CD26/DPPIV may interact with these biological factors (23, 44, 47). These findings imply that $CD26^+$ T cells play a role in the inflammation process and subsequent tissue damage in autoimmune diseases. Our results may thus provide a new approach to the treatment of autoimmune diseases or other immune-mediated disorders by directly interfering with activated T-cell and APC interaction. Moreover, targeting the interaction of the pocket structure of CD26 and the scaffolding domain of caveolin-1 may lead to novel therapeutic approaches utilizing agonists or antagonists that regulate antigen-specific immune response in not only immune-mediated disorders but also cancer immunotherapy and viral vaccination as strategies to enhance immune response (8).

ACKNOWLEDGMENTS

This work was supported by a grant-in-aid of the Ministry of Education, Science, Sports, and Culture and the Ministry of Health, Labor, and Welfare, Japan (K.O. and C.M.). N.H.D. is the recipient of a grant from the MD Anderson Cancer Center Physician-Scientist Program and the Gillson Longenbaugh Foundation.

REFERENCES

1. **Abreu, M. T., P. Vora, E. Faure, L. S. Thomas, E. T. Arnold, and M. Arditi.** 2001. Decreased expression of Toll-like receptor-4 and MD-2 correlates with intestinal epithelial cell protection against dysregulated proinflammatory gene expression in response to bacterial lipopolysaccharide. J. Immunol. **167**:1609–1616.
2. **Berberich, I., G. L. Shu, and E. A. Clark.** 1994. Cross-linking CD40 on B cells rapidly activates nuclear factor-kappa B. J. Immunol. **153**:4357–4366.
3. **Böl, G., O. J. Kreuzer, and R. Brigelius-Flohe.** 2000. Translocation of the interleukin-1 receptor-associated kinase-1 (IRAK-1) into the nucleus. FEBS Lett. **477**:73–78.
4. **Bucci, M., J. P. Gratton, R. D. Rudic, L. Acevedo, F. Roviezzo, G. Cirino, and W. C. Sessa.** 2000. In vivo delivery of the caveolin-1 scaffolding domain inhibits nitric oxide synthesis and reduces inflammation. Nat. Med. **6**:1362–1367.
5. **Burns, K., J. Clatworthy, L. Martin, F. Martinon, C. Plumpton, B. Maschera, A. Lewis, K. Ray, J. Tschopp, and F. Volpe.** 2000. Tollip, a new component of the IL-1RI pathway, links IRAK to the IL-1 receptor. Nat. Cell Biol. **2**:346–351.

6. **Burns, K., S. Janssens, B. Brissoni, N. Olivos, R. Beyaert, and J. Tschopp.** 2003. Inhibition of interleukin 1 receptor/Toll-like receptor signaling through the alternatively spliced, short form of MyD88 is due to its failure to recruit IRAK-4. J. Exp. Med. **197**:263–268.
7. **Cao, Z., W. J. Henzel, and X. Gao.** 1996. IRAK: a kinase associated with the interleukin-1 receptor. Science **271**:1128–1131.
8. **Carver, L. A., and J. E. Schnitzer.** 2003. Caveolae: mining little caves for new cancer targets. Nat. Rev. Cancer **3**:571–581.
9. **Choo, J. K., J. D. Seebach, V. Nickeleit, A. Shimizu, H. Lei, D. H. Sachs, and J. C. Madsen.** 1997. Species differences in the expression of major histocompatibility complex class II antigens on coronary artery endothelium: implications for cell-mediated xenoreactivity. Transplantation **64**:1315–1322.
10. **Cooke, E. L., I. J. Uings, C. L. Xia, P. Woo, and K. P. Ray.** 2001. Functional analysis of the interleukin-1-receptor-associated kinase (IRAK-1) in interleukin-1 beta-stimulated nuclear factor kappa B (NF-kappa B) pathway activation: IRAK-1 associates with the NF-kappa B essential modulator (NEMO) upon receptor stimulation. Biochem. J. **359**:403–410.
11. **Dang, N. H., Y. Torimoto, K. Shimamura, T. Tanaka, J. F. Daley, S. F. Schlossman, and C. Morimoto.** 1991. 1F7 (CD26): a marker of thymic maturation involved in the differential regulation of the CD3 and CD2 pathways of human thymocyte activation. J. Immunol. **147**:2825–2832.
12. **Dang, N. H., Y. Torimoto, K. Sugita, J. F. Daley, P. Schow, C. Prado, S. F. Schlossman, and C. Morimoto.** 1990. Cell surface modulation of CD26 by anti-1F7 monoclonal antibody. Analysis of surface expression and human T cell activation. J. Immunol. **145**:3963–3971.
13. **Dumonde, D. C., M. S. Pulley, F. J. Paradinas, B. M. Southcott, D. O'Connell, M. R. Robinson, F. den Hollander, and A. H. Schuurs.** 1982. Histological features of skin reactions to human lymphoid cell line lymphokine in patients with advanced cancer. J. Pathol. **138**:289–308.
14. **Eguchi, K., Y. Ueki, C. Shimomura, T. Otsubo, H. Nakao, K. Migita, A. Kawakami, M. Matsunaga, H. Tezuka, N. Ishikawa, et al.** 1989. Increment in the Ta1+ cells in the peripheral blood and thyroid tissue of patients with Graves' disease. J. Immunol. **142**:4233–4240.
15. **Feng, X., M. L. Gaeta, L. A. Madge, J. H. Yang, J. R. Bradley, and J. S. Pober.** 2001. Caveolin-1 associates with TRAF2 to form a complex that is recruited to tumor necrosis factor receptors. J. Biol. Chem. **276**:8341–8349.
16. **Fleischer, B.** 1994. CD26: a surface protease involved in T-cell activation. Immunol. Today **15**:180–184.
17. **Gerli, R., C. Muscat, A. Bertotto, O. Bistoni, E. Agea, R. Tognellini, G. Fiorucci, M. Cesarotti, and S. Bombardieri.** 1996. CD26 surface molecule involvement in T cell activation and lymphokine synthesis in rheumatoid and other inflammatory synovitis. Clin. Immunol. Immunopathol. **80**:31–37.
18. **Glenney, J. R., Jr.** 1989. Tyrosine phosphorylation of a 22-kDa protein is correlated with transformation by Rous sarcoma virus. J. Biol. Chem. **264**: 20163–20166.
19. **Hegen, M., J. Kameoka, R. P. Dong, S. F. Schlossman, and C. Morimoto.** 1997. Cross-linking of CD26 by antibody induces tyrosine phosphorylation and activation of mitogen-activated protein kinase. Immunology **90**:257–264.
20. **Ikushima, H., Y. Munakata, T. Ishii, S. Iwata, M. Terashima, H. Tanaka, S. F. Schlossman, and C. Morimoto.** 2000. Internalization of CD26 by mannose 6-phosphate/insulin-like growth factor II receptor contributes to T cell activation. Proc. Natl. Acad. Sci. USA **97**:8439–8444.
21. **Ishii, T., K. Ohnuma, A. Murakami, N. Takasawa, S. Kobayashi, N. H. Dang, S. F. Schlossman, and C. Morimoto.** 2001. CD26-mediated signaling for T cell activation occurs in lipid rafts through its association with CD45RO. Proc. Natl. Acad. Sci. USA **98**:12138–12143.
22. **Ishii, T., K. Ohnuma, A. Murakami, N. Takasawa, T. Yamochi, S. Iwata, M. Uchiyama, N. H. Dang, H. Tanaka, and C. Morimoto.** 2003. SS-A/Ro52, an autoantigen involved in CD28-mediated IL-2 production. J. Immunol. **170**: 3653–3661.
23. **Iwata, S., N. Yamaguchi, Y. Munakata, H. Ikushima, J. F. Lee, O. Hosono, S. F. Schlossman, and C. Morimoto.** 1999. CD26/dipeptidyl peptidase IV differentially regulates the chemotaxis of T cells and monocytes toward RANTES: possible mechanism for the switch from innate to acquired immune response. Int. Immunol. **11**:417–426.
24. **Kanakaraj, P., P. H. Schafer, D. E. Cavender, Y. Wu, K. Ngo, P. F. Grealish, S. A. Wadsworth, P. A. Peterson, J. J. Siekierka, C. A. Harris, and W. P. Fung-Leung.** 1998. Interleukin (IL)-1 receptor-associated kinase (IRAK) requirement for optimal induction of multiple IL-1 signaling pathways and IL-6 production. J. Exp. Med. **187**:2073–2079.
25. **Katoh, Y., Y. Shiba, H. Mitsuhashi, Y. Yanagida, H. Takatsu, and K. Nakayama.** 2004. Tollip and Tom1 form a complex and recruit ubiquitin-conjugated proteins onto early endosomes. J. Biol. Chem. **279**:24435–24443.
26. **Kobayashi, K., L. D. Hernandez, J. E. Galan, C. A. Janeway, Jr., R. Medzhitov, and R. A. Flavell.** 2002. IRAK-M is a negative regulator of Toll-like receptor signaling. Cell **110**:191–202.
27. **Kobayashi, S., K. Ohnuma, M. Uchiyama, K. Iino, S. Iwata, N. H. Dang, and C. Morimoto.** 2004. Association of CD26 with CD45RA outside lipid rafts attenuates cord blood T-cell activation. Blood **103**:1002–1010.
28. **Lei, M. G., and D. C. Morrison.** 2000. Differential expression of caveolin-1 in lipopolysaccharide-activated murine macrophages. Infect. Immun. **68**:5084–5089.
29. **Lenschow, D. J., A. I. Sperling, M. P. Cooke, G. Freeman, L. Rhee, D. C. Decker, G. Gray, L. M. Nadler, C. C. Goodnow, and J. A. Bluestone.** 1994. Differential up-regulation of the B7-1 and B7-2 costimulatory molecules after Ig receptor engagement by antigen. J. Immunol. **153**:1990–1997.
30. **Li, T., J. Hu, and L. Li.** 2004. Characterization of Tollip protein upon lipopolysaccharide challenge. Mol. Immunol. **41**:85–92.
31. **Li, X., M. Commane, C. Burns, K. Vithalani, Z. Cao, and G. R. Stark.** 1999. Mutant cells that do not respond to interleukin-1 (IL-1) reveal a novel role for IL-1 receptor-associated kinase. Mol. Cell. Biol. **19**:4643–4652.
32. **Makino, Y., H. Nakamura, E. Ikeda, K. Ohnuma, K. Yamauchi, Y. Yabe, L. Poellinger, Y. Okada, C. Morimoto, and H. Tanaka.** 2003. Hypoxia-inducible factor regulates survival of antigen receptor-driven T cells. J. Immunol. **171**:6534–6540.
33. **Masuyama, J., J. S. Berman, W. W. Cruikshank, C. Morimoto, and D. M. Center.** 1992. Evidence for recent as well as long term activation of T cells migrating through endothelial cell monolayers in vitro. J. Immunol. **148**: 1367–1374.
34. **Masuyama, J., T. Yoshio, K. Suzuki, S. Kitagawa, M. Iwamoto, T. Kamimura, D. Hirata, A. Takeda, S. Kano, and S. Minota.** 1999. Characterization of the 4C8 antigen involved in transendothelial migration of CD26(hi) T cells after tight adhesion to human umbilical vein endothelial cell monolayers. J. Exp. Med. **189**:979–990.
35. **McAdam, A. J., A. N. Schweitzer, and A. H. Sharpe.** 1998. The role of B7 co-stimulation in activation and differentiation of CD4+ and CD8+ T cells. Immunol. Rev. **165**:231–247.
36. **Mestas, J., and C. C. Hughes.** 2004. Of mice and not men: differences between mouse and human immunology. J. Immunol. **172**:2731–2738.
37. **Mizokami, A., K. Eguchi, A. Kawakami, H. Ida, Y. Kawabe, T. Tsukada, T. Aoyagi, K. Maeda, C. Morimoto, and S. Nagataki.** 1996. Increased population of high fluorescence 1F7 (CD26) antigen on T cells in synovial fluid of patients with rheumatoid arthritis. J. Rheumatol. **23**:2022–2026.
38. **Morimoto, C., and S. F. Schlossman.** 1998. The structure and function of CD26 in the T-cell immune response. Immunol. Rev. **161**:55–70.
39. **Morimoto, C., Y. Torimoto, G. Levinson, C. E. Rudd, M. Schrieber, N. H. Dang, N. L. Letvin, and S. F. Schlossman.** 1989. 1F7, a novel cell surface molecule, involved in helper function of CD4 cells. J. Immunol. **143**:3430–3439.
40. **Muscat, C., A. Bertotto, E. Agea, O. Bistoni, R. Ercolani, R. Tognellini, F. Spinozzi, M. Cesarotti, and R. Gerli.** 1994. Expression and functional role of 1F7 (CD26) antigen on peripheral blood and synovial fluid T cells in rheumatoid arthritis patients. Clin. Exp. Immunol. **98**:252–256.
41. **Naquet, P., H. R. MacDonald, P. Brekelmans, J. Barbet, S. Marchetto, W. Van Ewijk, and M. Pierres.** 1988. A novel T cell-activating molecule (THAM) highly expressed on CD4−CD8− murine thymocytes. J. Immunol. **141**:4101–4109.
42. **Ohnuma, K., Y. Munakata, T. Ishii, S. Iwata, S. Kobayashi, O. Hosono, H. Kawasaki, N. H. Dang, and C. Morimoto.** 2001. Soluble CD26/dipeptidyl peptidase IV induces T cell proliferation through CD86 up-regulation on APCs. J. Immunol. **167**:6745–6755.
43. **Ohnuma, K., T. Yamochi, M. Uchiyama, K. Nishibashi, N. Yoshikawa, N. Shimizu, S. Iwata, H. Tanaka, N. H. Dang, and C. Morimoto.** 2004. CD26 up-regulates expression of CD86 on antigen-presenting cells by means of caveolin-1. Proc. Natl. Acad. Sci. USA **101**:14186–14191.
44. **Ohtsuki, T., O. Hosono, H. Kobayashi, Y. Munakata, A. Souta, T. Shioda, and C. Morimoto.** 1998. Negative regulation of the anti-human immunodeficiency virus and chemotactic activity of human stromal cell-derived factor 1alpha by CD26/dipeptidyl peptidase IV. FEBS Lett. **431**:236–240.
45. **Oravecz, T., M. Pall, G. Roderiquez, M. D. Gorrell, M. Ditto, N. Y. Nguyen, R. Boykins, E. Unsworth, and M. A. Norcross.** 1997. Regulation of the receptor specificity and function of the chemokine RANTES (regulated on activation, normal T cell expressed and secreted) by dipeptidyl peptidase IV (CD26)-mediated cleavage. J. Exp. Med. **186**:1865–1872.
46. **Pober, J. S., M. S. Kluger, and J. S. Schechner.** 2001. Human endothelial cell presentation of antigen and the homing of memory/effector T cells to skin. Ann. N. Y. Acad. Sci. **941**:12–25.
47. **Proost, P., S. Struyf, D. Schols, G. Opdenakker, S. Sozzani, P. Allavena, A. Mantovani, K. Augustyns, G. Bal, A. Haemers, A. M. Lambeir, S. Scharpe, J. Van Damme, and I. De Meester.** 1999. Truncation of macrophage-derived chemokine by CD26/dipeptidyl-peptidase IV beyond its predicted cleavage site affects chemotactic activity and CC chemokine receptor 4 interaction. J. Biol. Chem. **274**:3988–3993.
48. **Razani, B., S. E. Woodman, and M. P. Lisanti.** 2002. Caveolae: from cell biology to animal physiology. Pharmacol. Rev. **54**:431–467.
49. **Sargiacomo, M., P. E. Scherer, Z. Tang, E. Kubler, K. S. Song, M. C. Sanders, and M. P. Lisanti.** 1995. Oligomeric structure of caveolin: implications for caveolae membrane organization. Proc. Natl. Acad. Sci. USA **92**:9407–9411.
50. **Shih, S. C., G. Prag, S. A. Francis, M. A. Sutanto, J. H. Hurley, and L. Hicke.** 2003. A ubiquitin-binding motif required for intramolecular monoubiquitylation, the CUE domain. EMBO J. **22**:1273–1281.
51. **Smart, E. J., G. A. Graf, M. A. McNiven, W. C. Sessa, J. A. Engelman, P. E.**

Scherer, T. Okamoto, and M. P. Lisanti. 1999. Caveolins, liquid-ordered domains, and signal transduction. Mol. Cell. Biol. **19:**7289–7304.
52. **Song, K. S., Z. Tang, S. Li, and M. P. Lisanti.** 1997. Mutational analysis of the properties of caveolin-1. A novel role for the C-terminal domain in mediating homo-typic caveolin-caveolin interactions. J. Biol. Chem. **272:** 4398–4403.
53. **Swantek, J. L., M. F. Tsen, M. H. Cobb, and J. A. Thomas.** 2000. IL-1 receptor-associated kinase modulates host responsiveness to endotoxin. J. Immunol. **164:**4301–4306.
54. **Sykes, M.** 2001. Mixed chimerism and transplant tolerance. Immunity **14:** 417–424.
55. **Tanaka, J., Y. Miwa, K. Miyoshi, A. Ueno, and H. Inoue.** 1999. Construction of Epstein-Barr virus-based expression vector containing mini-oriP. Biochem. Biophys. Res. Commun. **264:**938–943.
56. **Tanaka, T., D. Camerini, B. Seed, Y. Torimoto, N. H. Dang, J. Kameoka, H. N. Dahlberg, S. F. Schlossman, and C. Morimoto.** 1992. Cloning and functional expression of the T cell activation antigen CD26. J. Immunol. **149:**481–486.
57. **Tanaka, T., J. S. Duke-Cohan, J. Kameoka, A. Yaron, I. Lee, S. F. Schlossman, and C. Morimoto.** 1994. Enhancement of antigen-induced T-cell proliferation by soluble CD26/dipeptidyl peptidase IV. Proc. Natl. Acad. Sci. USA **91:**3082–3086.
58. **Tanaka, T., J. Kameoka, A. Yaron, S. F. Schlossman, and C. Morimoto.** 1993. The costimulatory activity of the CD26 antigen requires dipeptidyl peptidase IV enzymatic activity. Proc. Natl. Acad. Sci. USA **90:**4586–4590.
59. **Thomas, J. A., J. L. Allen, M. Tsen, T. Dubnicoff, J. Danao, X. C. Liao, Z. Cao, and S. A. Wasserman.** 1999. Impaired cytokine signaling in mice lacking the IL-1 receptor-associated kinase. J. Immunol. **163:**978–984.
60. **Yamin, T. T., and D. K. Miller.** 1997. The interleukin-1 receptor-associated kinase is degraded by proteasomes following its phosphorylation. J. Biol. Chem. **272:**21540–21547.
61. **Yamochi, T., I. Nishimoto, T. Okuda, and M. Matsuoka.** 2001. ik3-1/Cables is associated with Trap and Pctaire2. Biochem. Biophys. Res. Commun. **286:**1045–1050.
62. **Zhang, G., and S. Ghosh.** 2002. Negative regulation of Toll-like receptor-mediated signaling by Tollip. J. Biol. Chem. **277:**7059–7065.

Nedd9 Protein, a Cas-L Homologue, Is Upregulated After Transient Global Ischemia in Rats

Possible Involvement of Nedd9 in the Differentiation of Neurons After Ischemia

Takahiro Sasaki, MD, PhD; Satoshi Iwata, MD, PhD; Hirotaka James Okano, MD, PhD; Yasuyo Urasaki, MS; Junichi Hamada, MD, PhD; Hirotoshi Tanaka, MD, PhD; Nam H. Dang, MD, PhD; Hideyuki Okano, MD, PhD; Chikao Morimoto, MD, PhD

Background and Purpose—Some proteins involved in self-repair after stroke in the adult brain are primarily expressed during embryonic development and strongly down-regulated during the early postnatal phase. Neuronal precursor cell-expressed, developmentally down-regulated gene (Nedd) 9 was recognized to be identical to Crk-associated substrate lymphocyte type (Cas-L), a docking protein that associates with a variety of signaling molecules, such as focal adhesion kinase (FAK), proline-rich tyrosine kinase 2 (Pyk2), and Crk. We investigated the involvement of these proteins in the pathophysiology of global cerebral ischemia.

Methods—The mouse Cas-L/Nedd9 cDNAs were cloned. The expression and function of Cas-L/Nedd9 protein in the pathogenesis of global ischemia in rats was investigated by RT-PCR, Western blot analysis, and immunohistochemistry. The neurite outgrowth of the transfectants of Nedd9 deletion mutants in PC-12 cells was also assessed to clarify the function of the Nedd9 protein.

Results—Nedd9 was a splicing variant of Cas-L and was selectively induced in neurons of the cerebral cortex and hippocampus 1 to 14 days after the ischemia. Induced Nedd9 protein was tyrosine phosphorylated and was bound to FAK in dendrite and soma of neurons after the ischemia. Finally, it was demonstrated that Nedd9 promoted neurite outgrowth of PC-12 cells.

Conclusions—Our study may support the potential of Nedd9 for participation in the differentiation of neurons after global ischemia in rats. (***Stroke.* 2005;36:2457-2462.**)

Key Words: cerebral ischemia ■ global ■ rats ■ neural differentiation

Identification of an endogenous protein involved in self-repair after stroke in adult brain can potentially widen the therapeutic time window. Ischemia is a powerful reformatting and reprogramming stimulus for the brain, which induces endogenous proteins related to the pathophysiology of the injured brain.[1] Some of these proteins, such as neurocan,[2] Nedd2/Caspase2,[3] and GAP43,[4] are primarily expressed by neurons or glia during embryonic development and are strongly down-regulated during the early postnatal phase.

Nedd9 was initially identified as a neuronal precursor cell (NPC)-expressed, developmentally down-regulated gene in the mouse central nervous system. Gene expression of Nedd9 is detected in the embryonic brain of embryonal day (E) 10 and 14 and disappears in the adult mouse brain.[5] The product of Nedd9 was subsequently reported to be identical to the mouse Crk-associated substrate lymphocyte-type (Cas-L) according to the homology database (http://www.ncbi.nlm.nih.gov/), which is also known as human enhancer of filamentation 1 cloned by another group.[6] Human Cas-L was first identified by our group as a 105-kDa protein predominantly tyrosine phosphorylated by the ligation of β1 integrins in human leukemia H9 cells.[7] The major biological functions of Cas-L are the restoration of interleukin-2 production by costimulation with β1 integrins and T-cell receptor complex[8] and the enhancement of cell migration by the engagement of β1 integrins and T-cell receptor complex or β1 integrins alone.[9] To exert these functions, it is necessary that Cas-L is associated with focal adhesion kinase (FAK) or proline-rich tyrosine kinase 2 (Pyk2) and is tyrosine phosphorylated by these kinases.[10] Cas-L is a hematopoietic variant of p130Cas,[7]

Received June 26, 2004; final revision received December 8, 2004; accepted January 11, 2005.

From the Division of Clinical Immunology (T.S., S.I., Y.U., H.T., C.M.), Advanced Clinical Research Center, Institute of Medical Science, the University of Tokyo, Tokyo, Japan; the Departments of Physiology (H.J.O., H.O.) and Neurology (T.S., J.H.), Keio University School of Medicine; Core Research for Evolutional Science and Technology (H.J.O., H.O.), Japan Science and Technology Agency, Saitama, Japan; and the Department of Lymphoma/Myeloma (N.H.D.), MD Anderson Cancer Center, University of Texas, TX.

Correspondence to Chikao Morimoto, MD, PhD, Division of Clinical Immunology, Advanced Clinical Research Center, the Institute of Medical Science, the University of Tokyo, 4-6-1 Shirokanedai, Minato-ku, Tokyo 108-8639, Japan. E-mail morimoto@ims.u-tokyo.ac.jp

Stroke is available at http://www.strokeaha.org

DOI: 10.1161/01.STR.0000185672.10390.30

which was identified as a 130-kDa protein that is highly tyrosine phosphorylated in v-Src-[11] and v-Crk-transformed cells.[12] These proteins and Efs/Sin compose the Cas family, which has a conserved secondary structure with numerous protein-protein interactions, such as Src-homology 3 (SH3) domain, substrate domain, serine-rich domain, coiled-coil regions, helix-loop-helix domain, and COOH-terminal domain.[7,13] These structures feature a docking molecule, which interacts with a variety of signaling molecules, including FAK and Pyk2. The function of Cas-L/Nedd9 in relation to the pathogenesis of brain ischemia, as well as the expression in adult brain, remains unknown.

In the present study, we cloned the cDNAs of mouse Cas-L/Nedd9 and assessed the temporal profile of Cas-L/Nedd9, as well as its related molecules, such as p130Cas, FAK, and Pyk2, in the brain of rats with transient global ischemia. We also investigated its physiological function by using PC-12 cells transfected with Nedd9.

Methods

Antibodies and Reagents

Monoclonal antibodies (mAbs) against FAK, p130Cas, and Pyk2 were obtained from Transduction Laboratories. Antiphosphotyrosine antibody (4G10) was purchased from Upstate Biotechnology, Inc. A mAb to neuron-specific nuclear protein (NeuN) was from Chemicon International, and horseradish peroxidase-conjugated goat anti-mouse and anti-goat anti-rabbit antibodies were from Promega. Affinity-purified rabbit anti-mouse antibody was purchased from Jackson Laboratories. Production of polyclonal antibody specific to Cas-L was described previously.[14] Protein A sepharose beads were from Pharmacia Biotech. All of the other reagents were purchased from Sigma-Aldrich unless otherwise stated.

cDNA Cloning of Murine Cas-L/Nedd9

A λgt11 human placenta cDNA library (Clontech Laboratories) was screened by hybridization with a ^{32}P-labeled probe for human Cas-L cDNA, which was labeled with [α-^{32}P] dCTP by the random primer labeling method, for 16 hours at 50°C in a solution of 50 mmol/L Tris-HCl, pH 7.5, 1 mol/L NaCl, 1% SDS, and 100 μg/mL sonicated salmon testis DNA, and then washed at 65°C in 0.1×SSC containing 1% SDS.[15] The hybridization-positive clones were sequenced by an ABI Dideoxy Terminator Cycle Sequencing kit.

Animals

Male Sprague-Dawley rats weighing 250 to 350 g were anesthetized by an IP injection of pentobarbital sodium (40 mg/kg). Twenty-one minutes of global ischemia were induced by occlusion of both common arteries with systemic hypotension <50 mm Hg.[16] The rectal temperature was continuously monitored and maintained at 37.0°C to 37.5°C with a thermostatically controlled heating pad. The experimental committee of Keio University approved the experimental protocol as meeting the experimental animal guidelines of Keio University School of Medicine.

RT-PCR

RT-PCR was performed using ISOGEN agent and BcaBEST RNA PCR kit (Takara Bio, Inc) with the following primers: forward 5′-AAATGTGGGCGAGGAAT-3′ for rat Nedd9, 5′-AGGGCTCATCTGACCAC-3′ for rat Cas-L, and reverse 5′-TGACTGGAGGGCTCTTG-3′ for both cDNAs. PCR cycles were as follows: 94°C, 1 minute; 55.6°C, 1 minute; and 72°C, 2 minutes (30 cycles).

Immunoprecipitation and Immunoblotting

Tissues of cerebral cortex and hippocampus were homogenized in suspension buffer (20 mmol/L HEPES-KOH, pH 7.5, 250 mmol/L sucrose, 10 mmol/L KCl, 1.5 mmol/L $MgCl_2$, 1 mmol/L EDTA, 1 mmol/L EGTA, 1 mmol/L dithiothreitol, 0.1 mmol/L phenylmethylsulfonyl fluoride, 2 μg/mL aprotinin, 10 μg/mL leupeptin, and 5 μg/mL pepstatin A). The lysates were immunoprecipitated with anti–Cas-L polyclonal antibody and protein A sepharose beads. The samples were separated by 8% SDS-PAGE and electrotransferred onto polyvinylidene difluoride membranes (Millipore). For immunoblotting, the primary antibodies and their dilutions were as follows: anti–Cas-L polyclonal antibody (1:2500), anti-Pyk2 mAb (1:2500), anti-FAK mAb (1:2000), anti p130Cas mAb (1:2500), and anti–β-actin mAb (1:5000).

Histological Examinations

Anesthetized rats were perfused transcardially with heparinized saline followed by 4% paraformaldehyde/PBS for tissue fixation, and paraffinized sections were made. The paraffinized sections (10 μm) were dewaxed and permeabilized with 0.1% Triton X-100/PBS and then blocked in 4% FBS/PBS. The primary antibodies and their dilutions were as follows: anti–Cas-L rabbit polyclonal antibody, 1:200; anti-FAK mAb, 1:200; and NeuN, 1:200. The sections were finally exposed to 0.025% diaminobenzidine and 0.075% H_2O_2 in PBS for 1 minute. For immunofluorescence staining, fluorescein isothiocyanate or Texas Red-conjugated anti-rabbit or anti-mouse IgG antibodies at 1:100 were used as the secondary antibody.

Gene Transfer Using Retrovirus

Retroviral gene transfer was carried out using the ping-pong infection method using Plat-E cells,[17] PT-67 cells (Clontech), and Fugene6 reagent (Roche Diagnostics) with pMX-Nedd9 wild type-IRES-GFP, pMX-Nedd9 SH3-IRES-GFP, pMX-Nedd9 F-IRES-GFP, pMX-Nedd9 δ SH3-IRES-GFP, pMX-Nedd9 δ SD-IRES-GFP, or pMX-IRES-GFP. The supernatants of PT-67 infected with each retrovirus were used to infect PC-12 cells.

Assessment of Neurite Outgrowth of PC-12 Cells

Infected PC-12 cells were cultured in DMEM plus 10% fetal calf serum and 5% horse serum. For the examination of neuritogenesis, 2.5×10^4 cells were seeded per 35-mm plate, grown overnight, and starved (0.5% FCS plus 0.5% horse serum) for 16 to 20 hours, then 50 ng/mL nerve growth factor (NGF) was added. After 6 days of stimulation, neurite length was measured on photographed fields containing 50 to 100 cells. Data were expressed in 2 ways: first, as the neurite length averaged over diameter of soma (bar diagrams; y axis=cell diameters); and second, as the number of neurites per cell. The level of statistical significance was assessed by ANOVA followed by Scheffé's post hoc test. Statistical significance was set at $P<0.01$.

Results

Cloning of Mouse Cas-L Revealed That Cas-L Was a Splicing Variant of Nedd9 With Identical Functional Domains

Using the cloned mouse Cas-L-related cDNAs, a sequence homology search was performed against the cDNA and genomic database. Nedd9 was found to share high degrees of homology with mouse Cas-L: 98.9% in nucleotide sequence and 98.6% in amino acid sequence (Figure 1a). An analysis of mouse genomic database revealed that Cas-L (MKYK-) was a splicing variant of Nedd9 (MWAR-), and the functional domains of these proteins were identical to each other. A homology search against a rat genomic database showed that the deduced amino acid sequences of mouse and rat Nedd9 were highly conserved between these species: 92.7% in the